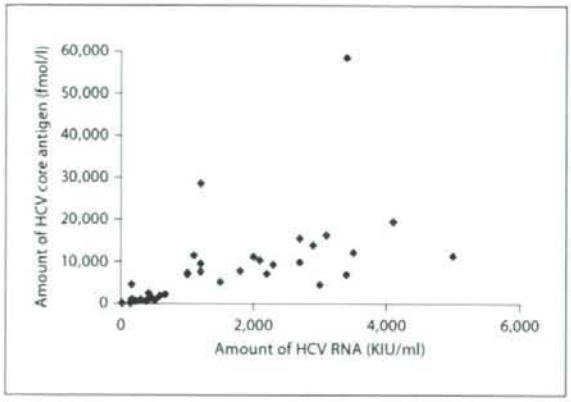

Fig. 1. Correlation between the amount of HCV core antigen and the amount of HCV RNA at the start of PEG-IFN/RBV combination therapy. There was a significant positive correlation (r^2 = 0.648, p = 0.0002. y = 4.48x + 1,470).

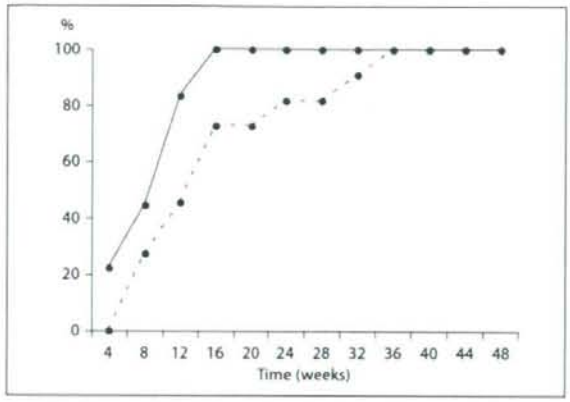

Fig. 2. Time course of HCV RNA eradication during PEG-IFN/RBV combination therapy. No significant difference was observed between SVR (——) and PR (- - -).

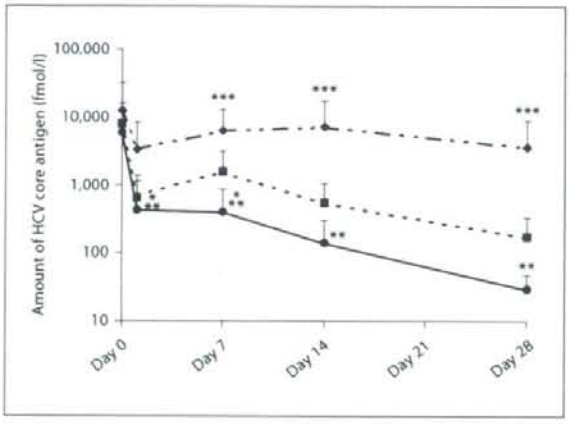

Fig. 3. Amount of HCV core antigen during PEG-IFN/RBV combination therapy. —— = SVR; - - - = PR; - -- - -- = NR. * $p < 0.05$, SVR vs. PR; ** $p < 0.05$, SVR vs. NR, and *** $p < 0.05$, NR vs. PR.

Four weeks after the start of therapy, the following reductions in the amount of HCV core antigen were observed: a 1-log reduction in 20% (2/10) of the NR group, in 91% (10/11) of the PR group and in 88.9% (16/18) of the SVR group, and a 2-log reduction in 0% (0/10) of the NR group, in 63.6% (7/11) of the PR group and in 55.6% (10/18) of the SVR group (table 2).

Discussion

HCV core antigen, first detected in the circulation of HCV-infected hosts by EIA-based methods [13], had some limitations, in that levels under 20 fmol/l of HCV RNA could not be detected. Consequently, the methods were limited to the monitoring of late events during and after antiviral treatment. A modified version of the EIA developed for HCV core antigen [11] easily exposes the epitope of HCV core antigen, and the binding by anti-HCV core antibody in the serum can be reduced by incubation with three types of detergents. Since the modified EIA requires only one pretreatment step, it is simpler than the first-generation versions; moreover, it is 100-fold more sensitive. The second-generation EIA for HCV core antigen is useful in the diagnosis of acute and chronic hepatitis C and in predicting and monitoring the effect of IFN treatment [14].

Recently, a new IRM assay-based test for detecting HCV core antigen, a further modification of the EIA method of Aoyagi et al. [11], overcomes the effects of the serological HCV genotype group at the level of HCV core antigen detectable by EIA in serum. The sensitivity and specificity of the IRM assay are 96.4 and 100%, respectively. The sensitivity is similar between HCV serotype I (HCV genotypes 1a and 1b; 97.6%) and HCV serotype II (HCV genotypes 2a and 2b; 94.0%) [12].

Furthermore, the cost of the IRM assay kit is less than one third of the RT-PCR assay. Thus, this new IRM assay

Table 1. Host-dependent, virus-related profile

	NR	PR	SVR	p
Gender, males/females	6/4	7/4	9/9	NS
Age, years	59.8 ± 9.9	63.5 ± 7.3	55.5 ± 9.4	NS
HCV RNA level, KIU/ml	1,185 ± 1,154	2,093 ± 1,355	1,328 ± 1,321	NS
HCV core antigen, fmol/l	12,781 ± 18,444	7,875 ± 3,418	5,809 ± 5,919	NS
Body weight, kg	61.2 ± 11.2	60.8 ± 14.5	57.5 ± 9.6	NS
Treatment history (retreatment/naïve)	6/4	4/7	7/11	NS
Body mass index	23.7 ± 3.7	22.7 ± 3.7	22.4 ± 9.6	NS
F0–1/F2–3	3/6	1/6	14/3	0.003

is an economically valuable option for monitoring the amount of HCV in patients with chronic HCV infection. Indeed, in our study, there was a strong correlation between the amount of HCV core antigen in serum by the IRM assay and the amount of HCV RNA in serum measured by quantitation RT-PCR ($r^2 = 0.648$).

Although some studies have suggested that quantitative HCV RNA determinations allow earlier assessment of treatment response, the assays were not generally available commercially, and they were not standardized. Therefore, we used the IRM assay to predict virological response during PEG-IFN/RBV therapy in patients with HCV-1b ≥100 KIU/ml.

To be able to assess whether long-term response is attainable as early as possible during the treatment course, and to have the option of discontinuing treatment in cases where virological response is not expected, is desirable. This strategy has the potential of making a trial more appealing to patients by providing a limited 'test' period of treatment before committing to a full course of therapy [6].

The accuracy of the degree of viral inhibition, during the early weeks of treatment (early virological response: EVR) with PEG-IFNα-2b/RBV, has been examined to identify patients who would not respond to therapy. The best definition of EVR is a reduction in HCV RNA by at least 2 log after the first 12 weeks of treatment compared with baseline. Depending on the treatment regimen, between 69 and 76% of patients have achieved this threshold, with SVR attained in 67–80% [15].

The importance of EVR has been emphasized in predicting SVR and non-SVR: patients who do not reach EVR are not responsive to further therapy. Discontinuation of treatment in patients not reaching EVR would reduce drug costs by >20%; consequently, early confirmation of viral reduction after initiating antiviral therapy for chronic hepatitis C is worthwhile [16].

Table 2. Reduction in the amount of HCV RNA 4 weeks after the start of PEG-IFN/RBV therapy

Reduction	NR	PR	SVR
1 log	20% (2/10)	91% (10/11)	88.9% (16/18)
2 log	0% (0/10)	63.6% (7/11)	55.6% (10/18)

Treatment with IFN results in a decline in HCV RNA levels, which can be resolved mathematically into two phases. The first-phase decline is usually measured at 24 or 48 h, and probably reflects direct inhibition of intracellular HCV production and release [17], with IFN efficacy ranging from about 70% (approximately 0.7 log units) for standard IFN given three times a week to more than 90% (1 log units) for high daily doses of standard IFN or PEG-IFN once a week [18, 19]. The second-phase decline begins after 24–48 h, is slower and more variable than the first phase, and is thought to reflect continued inhibition of replication and the gradual elimination of virus-infected cells [17]. The decay correlates less with the IFN dose than the first phase, but is more rapid with PEG-IFN as compared with standard IFN preparations [16].

Lowering HCV RNA during the first phase is essential for efficient elimination of HCV during the second phase. Decreases in HCV RNA titers within the first 24–48 h after the start of IFN, therefore, would be dependable estimates of antiviral efficacy [18, 19].

As observed with the first phase, RBV does not appear to influence second-phase kinetics [16]. Four weeks after

the start of therapy, a 1-log reduction was observed in 20% (2/10) of NR patients, 91% (10/11) of PR and 88.9% (16/18) of SVR, and a 2-log reduction in 0% (0/10) of NR, 63.6% (7/11) of PR and 55.6% (10/18) of SVR patients. These results indicate that the reduction of 1 and 2 log in the amount of HCV core antigen 4 weeks after therapy is not a defining condition for PR and SVR. There are two kinds of non-SVR (PR and NR): PR is defined as HCV RNA undetectable at the end of treatment and positive 24 weeks after the discontinuation of therapy; NR is defined as HCV RNA detectable at the end of treatment.

At all points of time, a significant difference was observed in the amount of HCV core antigen between SVR and NR. Accordingly, SVR can easily be differentiated from NR by IRM assay during therapy. With regard to the time course of HCV RNA eradication, however, there is no difference between PR and SVR. The prediction of SVR and PR by the earliest possible use of the IRM assay is desirable.

In our study, 1 and 7 days after the start of therapy, there was a significant difference in the amount of HCV core antigen between SVR and PR. Our finding that SVR and PR could be differentiated by the IRM assay during the first and second phases is very useful for clinicians engaged in the treatment of C-type hepatitis, because PR patients should be treated for 72 weeks in order to maximize the probability of SVR [20, 21].

Taken together, our results demonstrate that early viral dynamics, such as changes in the amount of HCV core antigen detected by the IRM assay in the first and second phases during PEG-IFNα-2b/RBV therapy, predict outcome not only between SVR and NR but also between SVR and PR. Since the number of patients was small in our study, further studies including larger patient cohorts are needed to confirm the promising potential of the IRM assay.

In conclusion, this new IRM assay is useful in predicting virological response during PEG-IFN/RBV combination therapy administered for chronic hepatitis C with high viral loads of HCV RNA genotype 1b.

Acknowledgments

This study was also carried out as part of the Program of Founding Research Centers for Emerging and Reemerging Infectious Diseases. We are indebted to K. Ohyama and Y. Kawamura for their assistance in the preparation of the manuscript.

Disclosure Statements

The authors have no disclosures to make.

References

1 Fried MW, Shiffman ML, Reddy KR, Smith C, Marinos G, Goncales FL Jr, Haussinger D, Diago M, Carosi G, Dhumeaux D, Craxi A, Lin A, Hoffman J, Yu J: Peginterferon alfa-2a plus ribavirin for chronic hepatitis C virus infection. N Engl J Med 2002;26:975–982.

2 Manns MP, McHutchison JG, Gordon SC, Rustgi VK, Shiffman M, Reindollar R, Goodman ZD, Koury K, Ling M, Albrecht JK: Peginterferon alfa-2b plus ribavirin compared with interferon alfa-2b plus ribavirin for initial treatment of chronic hepatitis C: randomized trial. Lancet 2001;22:958–965.

3 Nakamura H: Early prediction of sustained viral responder and non-responder during interferon and ribavirin combination therapy in chronic hepatitis C. Hepatol Res 2005; 33:269–271.

4 El-Shamy A, Sasayama M, Nagano-Fujii M, Sasase N, Imoto S, Kim SR, Hotta H: Prediction of efficient virological response to pegylated interferon/ribavirin combination therapy by NS5A sequences of hepatitis C virus and anti-NS5A antibodies in pre-treatment sera. Microbiol Immunol 2007;51:471–482.

5 Enomoto N, Sakuma I, Asahina Y, Kurosaki M, Murakami T, Yamamoto C, Ogura Y, Izumi N, Marumo F, Sato C: Mutations in the nonstructural protein 5A gene and response to interferon in patients with chronic hepatitis C virus 1b infection. N Engl J Med 1996; 334:77–81.

6 Akuta N, Suzuki S, Kawamura Y, Yatsuji H, Sezaki H, Suzuki Y, Hosaka T, Kobayashi M, Kobayashi M, Arase Y, Ikeda K, Miyakawa Y, Kumada H: Prediction of response to pegylated interferon and ribavirin in hepatitis C by polymorphism in the viral core protein and very early dynamics of viremia. Intervirology 2007;50:361–368.

7 Ferenci P: Predictors of response to therapy for chronic hepatitis C. Semin Liver Dis 2004;24:S25–S31.

8 Dickson RC, Mizokami M, Orito E, Qian KP, Lau JY: Quantification of serum HCV core antigen by a fluorescent enzyme immunoassay in liver transplant recipients with recurrent hepatitis C – clinical and virologic implications. Transplantation 1999;68:1512–1516.

9 Komatsu F, Takahashi K: Determination of serum hepatitis C (HCV) core protein using a novel approach for quantitative evaluation of HCV viremia in anti-HCV-positive patients. Liver 1999;19:375–380.

10 Widell A, Molnegren V, Pieksma F, Calmann M, Peterson J, Lee SR: Detection of hepatitis C core antigen in serum or plasma as a marker of hepatitis C viremia in the serological window-phase. Transfus Med 2002;12:107–113.

11 Aoyagi K, Ohue C, Iida K, Kimura T, Tanaka E, Kiyosawa K, Yagi S: Development of a simple and highly sensitive enzyme immunoassay for hepatitis C virus core antigen. J Clin Microbiol 1999;37:1802–1808.

12 Hayashi K, Hasuike S, Kusumoto K, Ido A, Uto H, Kenji N, Kohara M, Stuver SO: Usefulness of a new immuno-radiometric assay to detect hepatitis C core antigen in a community-based population. J Viral Hepat 2005;12:106–110.

13 Tanaka T, Lau JYN, Mizokami M, Orito E, Tanaka E, Kiyosawa K, Yasui K, Ohta Y, Hasegawa A, Tanaka S, et al: Simple fluorescent enzyme immunoassay for detection and quantification of hepatitis C viremia. J Hepatol 1995;23:742–745.
14 Tanaka E, Ohue C, Aoyagi K, Yamaguchi K, Yagi S, Kiyosawa K, Alter HJ: Evaluation of a new enzyme immunoassay for hepatitis C virus (HCV) core antigen with clinical sensitivity approximating that of genomic amplification of HCV RNA. Hepatology 2000;32:388–393.
15 Davis GL, Wong JB, McHutchison JG, Manns MP, Harvey J, Albrecht J: Early virologic response to treatment with peginterferon alfa 2b plus ribavirin in patients with chronic hepatitis C. Hepatology 2003;38:645–652.
16 Davis GL: Monitoring of viral levels during therapy of hepatitis C. Hepatology 2002;36:S145–S151.
17 Neumann AU, Lam NP, Dahari H, Gretch DR, Wiley TE, Layden TJ, Perelson AS: Hepatitis C viral dynamics in vivo and the antiviral efficacy of interferon-α therapy. Science 1998;282:103–107.
18 Lam NP, Neumann AU, Gretch DR, Wiley TE, Perelson AS, Layden TJ: Dose-dependent acute clearance of hepatitis C genotype 1 virus with interferon alfa. Hepatology 1997;26:226–231.
19 Zeuzem S, Herrmann E, Lee JH, Fricke J, Neumann AU, Modi M, Colucci G, Roth WK: Viral kinetics in patients with chronic hepatitis C treated with standard or peginterferon alfa-2a. Gastroenterology 2001;120:1438–1447.
20 Buti M, Valdes A, Sanchez-Avila F, Esteban R, Lurie Y: Extending combination therapy with peginterferon alfa-2b plus ribavirin for genotype 1 chronic hepatitis C late responders: a report of 9 cases. Hepatology 2003;37:1226–1227.
21 Berg T, von Wagner M, Nasser S, Sarrazin C, Heintges T, Gerlach T, Buggisch P, Goeser T, Rasenack J, Pape GR, Schmidt WE, Kallinowski B, Klinker H, Spingler U, Martus P, Alshuth U, Zeuzem S: Extended treatment duration for hepatitis C virus type 1: comparing 48 versus 72 weeks of peginterferon-alfa-2a plus ribavirin. Gastroenterology 2006;130:1086–1097.

JOURNAL OF VIROLOGY, Mar. 2009, p. 2389–2392
0022-538X/09/$08.00+0 doi:10.1128/JVI.01690-08

Vol. 83, No. 5

Proteasomal Turnover of Hepatitis C Virus Core Protein Is Regulated by Two Distinct Mechanisms: a Ubiquitin-Dependent Mechanism and a Ubiquitin-Independent but PA28γ-Dependent Mechanism▽

Ryosuke Suzuki,[1] Kohji Moriishi,[2] Kouichirou Fukuda,[1] Masayuki Shirakura,[1] Koji Ishii,[1] Ikuo Shoji,[3] Takaji Wakita,[1] Tatsuo Miyamura,[1] Yoshiharu Matsuura,[2] and Tetsuro Suzuki[1]*

Department of Virology II, National Institute of Infectious Diseases, Tokyo 162-8640,[1] Department of Molecular Virology, Research Institute for Microbial Diseases, Osaka University, Osaka 565-0871,[2] and Division of Microbiology, Kobe University Graduate School of Medicine, Hyogo 650-0017,[3] Japan

Received 8 August 2008/Accepted 5 December 2008

We have previously reported on the ubiquitylation and degradation of hepatitis C virus core protein. Here we demonstrate that proteasomal degradation of the core protein is mediated by two distinct mechanisms. One leads to polyubiquitylation, in which lysine residues in the N-terminal region are preferential ubiquitylation sites. The other is independent of the presence of ubiquitin. Gain- and loss-of-function analyses using lysineless mutants substantiate the hypothesis that the proteasome activator PA28γ, a binding partner of the core, is involved in the ubiquitin-independent degradation of the core protein. Our results suggest that turnover of this multifunctional viral protein can be tightly controlled via dual ubiquitin-dependent and -independent proteasomal pathways.

Hepatitis C virus (HCV) core protein, whose amino acid sequence is highly conserved among different HCV strains, not only is involved in the formation of the HCV virion but also has a number of regulatory functions, including modulation of signaling pathways, cellular and viral gene expression, cell transformation, apoptosis, and lipid metabolism (reviewed in references 9 and 15). We have previously reported that the E6AP E3 ubiquitin (Ub) ligase binds to the core protein and plays an important role in polyubiquitylation and proteasomal degradation of the core protein (22). Another study from our group identified the proteasome activator PA28γ/REG-γ as an HCV core-binding partner, demonstrating degradation of the core protein via a PA28γ-dependent pathway (16, 17). In this work, we further investigated the molecular mechanisms underlying proteasomal degradation of the core protein and found that in addition to regulation by the Ub-mediated pathway, the turnover of the core protein is also regulated by PA28γ in a Ub-independent manner.

Although ubiquitylation of substrates generally requires at least one Lys residue to serve as a Ub acceptor site (5), there is no consensus as to the specificity of the Lys targeted by Ub (4, 8). To determine the sites of Ub conjugation in the core protein, we used site-directed mutagenesis to replace individual Lys residues or clusters of Lys residues with Arg residues in the N-terminal 152 amino acids (aa) of the core (C152), within which is contained all seven Lys residues (Fig. 1A). Plasmids expressing a variety of mutated core proteins were generated by PCR and inserted into the pCAGGS (18). Each core-expressing construct was transfected into human embryonic kidney 293T cells along with the pMT107 (25) encoding a Ub moiety tagged with six His residues (His_6). Transfected cells were treated with the proteasome inhibitor MG132 for 14 h to maximize the level of Ub-conjugated core intermediates by blocking the proteasome pathway and were harvested 48 h posttransfection. His_6-tagged proteins were purified from the extracts by Ni^{2+}-chelation chromatography. Eluted protein and whole lysates of transfected cells before purification were analyzed by Western blotting using anticore antibodies (Fig. 1B). Mutations replacing one or two Lys residues with Arg in the core protein did not affect the efficiency of ubiquitylation: detection of multiple Ub-conjugated core intermediates was observed in the mutant core proteins comparable to the results seen with the wild-type core protein as previously reported (23). In contrast, a substitution of four N-terminal Lys residues (C152K6-23R) caused a significant reduction in ubiquitylation (Fig. 1B, lane 9). Multiple Ub-conjugated core intermediates were not detected in the Lys-less mutant (C152KR), in which all seven Lys residues were replaced with Arg (Fig. 1B, lane 11). These results suggest that there is not a particular Lys residue in the core protein to act as the Ub acceptor but that more than one Lys located in its N-terminal region can serve as the preferential ubiquitylation site. In rare cases, Ub is known to be conjugated to the N terminus of proteins; however, these results indicate that this does not occur within the core protein.

To investigate how polyubiquitylation correlates with proteasome degradation of the core protein, we performed kinetic analysis of the wild-type and mutated core proteins by use of the Ub protein reference (UPR) technique, which can compensate for data scatter of sample-to-sample variations such as levels of expression (10, 24). Fusion proteins expressed from UPR-based constructs (Fig. 2A) were cotranslationally cleaved by deubiquitylating enzymes, thereby generating equimolar quantities of the core proteins and the reference protein, dihydrofolate reductase-hemagglutinin (DHFR-HA) tag-modified Ub, in which the Lys at aa 48 was replaced by Arg to prevent its polyubiquitylation (Ub^{R48}). After 24 h of transfec-

* Corresponding author. Mailing address: Department of Virology II, National Institute of Infectious Diseases, 1-23-1 Toyama, Shinjuku-ku, Tokyo 162-8640, Japan. Phone: 81-3-5285-1111. Fax: 81-3-5285-1161. E-mail: tesuzuki@nih.go.jp.

▽ Published ahead of print on 17 December 2008.

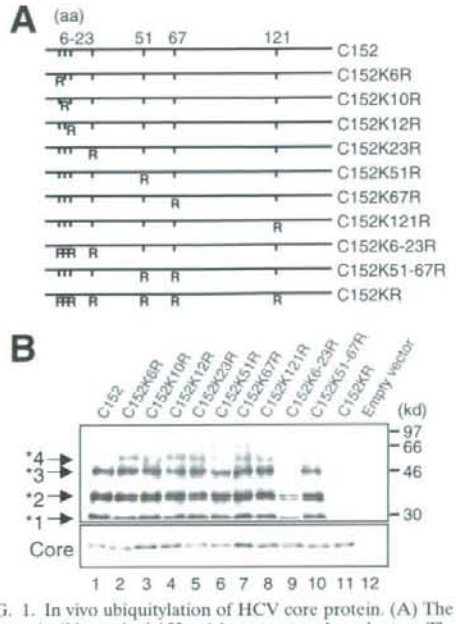

FIG. 1. In vivo ubiquitylation of HCV core protein. (A) The HCV core protein (N-terminal 152 aa) is represented on the top. The positions of the amino acid residues of the core protein are indicated above the bold lines. The positions of the seven Lys residues in the core are marked by vertical ticks. Substitution of Lys with Arg (R) is schematically depicted. (B) Detection of ubiquitylated forms of the core proteins. The transfected cells with core expression plasmids and pMT107 were treated with the proteasome inhibitor MG132 and harvested 48 h after transfection. His_6-tagged proteins were purified and subsequently analyzed by Western blot analysis using anticore antibody (upper panel). Core proteins conjugated to a number of His_6-Ub are denoted with asterisks. Whole lysates of transfected cells before purification were also analyzed (lower panel). Lanes 1 to 11, C152 to C152KR, as indicated for panel A. Lane 12; empty vector.

tion with UPR constructs, cells were treated with cycloheximide and the amounts of core proteins and DHFR-HA-Ub^{R48} at the indicated time points were determined by Western blot analysis using anticore and anti-HA antibodies. The mature form of the core protein, aa 1 to 173 (C173) (13, 20), and C152 were degraded with first-order kinetics (Fig. 2B and D). MG132 completely blocked the degradation of C173 and C152 (Fig. 2B), and C152K6-23R and C152KR were markedly stabilized (Fig. 2C). The half-lives of C173 and C152 were calculated to be 5 to 6 h, whereas those of C152K6-23R and C152KR were calculated to be 22 to 24 h (Fig. 2D), confirming that the Ub plays an important role in regulating degradation of the core protein. Nevertheless, these results also suggest possible involvement of the Ub-independent pathway in the turnover of the core protein, as C152KR is more destabilized than the reference protein (Fig. 2C and 2D).

We have shown that PA28γ specifically binds to the core protein and is involved in its degradation (16, 17). Recent studies demonstrated that PA28γ is responsible for Ub-independent degradation of the steroid receptor coactivator SRC-3 and cell cycle inhibitors such as p21 (3, 11, 12). Thus, we next investigated the possibility of PA28γ involvement in the degradation of either C152KR or C152. Since C152KR carries two amino acid substitutions in the PA28γ-binding region (aa 44 to 71) (17), we tested the influence of the mutations of C152KR on the interaction with PA28γ by use of a coimmunoprecipi-

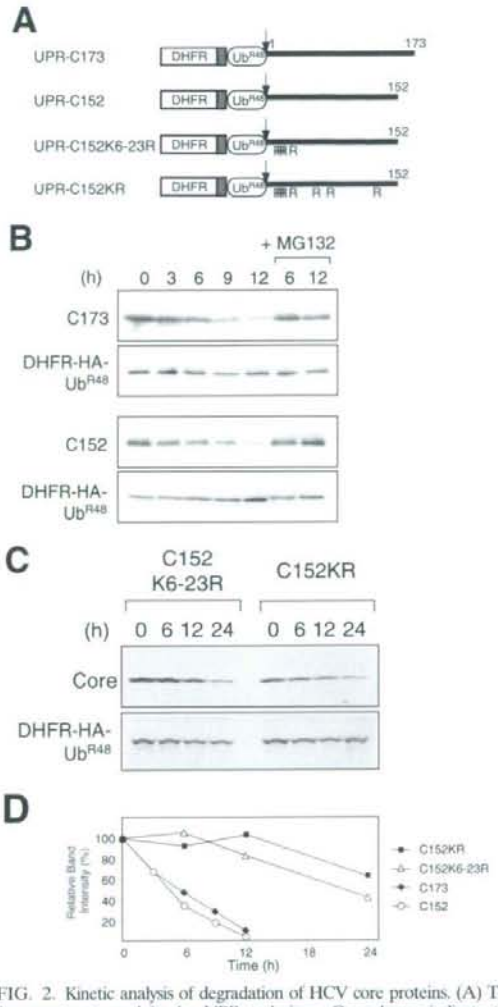

FIG. 2. Kinetic analysis of degradation of HCV core proteins. (A) The fusion constructs used in the UPR technique. Open boxes indicate the DHFR sequence, which is extended at the C terminus by a sequence containing the HA epitope (hatched boxes). Ub^{R48} moieties bearing the Lys-Arg substitution at aa 48 are represented by open ellipses. Bold lines indicate the regions of the core protein. The amino acid positions of the core protein are indicated above the bold lines. The arrows indicate the sites of in vivo cleavage by deubiquitylating enzymes. (B and C) Turnover of the core proteins. After a 24-h transfection with each UPR construct, cells were treated with 50 μg of cycloheximide/ml in the presence or absence of 10 μM MG132 for the different time periods indicated. Cells were lysed at the different time points indicated, followed by evaluation via sodium dodecyl sulfate-polyacrylamide gel electrophoresis and Western blot analysis using antibodies against the core protein and HA. (D) Quantitation of the data shown in panels B and C. At each time point, the ratio of band intensity of the core protein relative to the reference DHFR-HA-Ub^{R48} was determined by densitometry and is plotted as a percentage of the ratio at time zero.

tation assay. When Flag-tagged PA28γ (F-PA28γ) was expressed in cells along with C152 or C152KR, F-PA28γ precipitated along with both C152 and C152KR, indicating that PA28γ interacts with both core proteins (Fig. 3A). Figure 3B reveals the effect of exogenous expression of F-PA28γ on the steady-state levels of C152 and C152KR. Consistent with previous data (17), the expression level of C152 was decreased to a nearly undetectable level in the presence of PA28γ (Fig. 3B, lanes 1 and 3). Interestingly, exogenous expression of PA28γ led to a marked reduction in the amount of C152KR expressed (Fig. 3B, lanes 5 and 7). Treatment with MG132 increased the steady-state level of the C152KR in the presence of F-PA28γ as well as the level of C152 (Fig. 3B, lanes 4 and 8).

We further investigated whether PA28γ affects the turnover of Lys-less core protein through time course experiments. C152KR was rapidly destabilized and almost completely degraded in a 3-h chase experiment using cells overexpressing F-PA28γ (Fig. 3C, left panels). A similar result was obtained using an analogous Lys-less mutant of the full-length core protein C191KR (Fig. 3C, right panels), thus demonstrating that the Lys-less core protein undergoes proteasomal degradation in a PA28γ-dependent manner. These results suggest that PA28γ may play a role in accelerating the turnover of the HCV core protein that is independent of ubiquitylation.

Finally, we examined gain- and loss-of-function of PA28γ with respect to degradation of full-length wild-type (C191) and mutated (C191KR) core proteins in human hepatoma Huh-7 cells. As expected, exogenous expression of PA28γ or E6AP caused a decrease in the C191 steady-state levels (Fig. 4A). In contrast, the C191KR level was decreased with expression of PA28γ but not of E6AP. We further used RNA interference to inhibit expression of PA28γ or E6AP. An increase in the abundance of C191KR was observed with PA28γ small interfering RNA (siRNA) but not with E6AP siRNA (Fig. 4B). An increase in the C191 level caused by the activity of siRNA against PA28γ or E6AP was confirmed as well.

Taking these results together, we conclude that turnover of the core protein is regulated by both Ub-dependent and Ub-independent pathways and that PA28γ is possibly involved in Ub-independent proteasomal degradation of the core protein. PA28 is known to specifically bind and activate the 20S proteasome (19). Thus, PA28γ may function by facilitating the delivery of the core protein to the proteasome in a Ub-independent manner.

Accumulating evidence suggests the existence of proteasome-dependent but Ub-independent pathways for protein degradation, and several important molecules, such as p53, p73, Rb, SRC-3, and the hepatitis B virus X protein, have two distinct degradation pathways that function in a Ub-dependent and Ub-independent manner (1, 2, 6, 7, 14, 21, 27). Recently, critical roles for PA28γ in the Ub-independent pathway have been demonstrated; SRC-3 and p21 can be recognized by the 20S proteasome independently of ubiquitylation through their interaction with PA28γ (3, 11, 12). It has also been reported that phosphorylation-dependent ubiquitylation mediated by GSK3 and SCF is important for SRC-3 turnover (26). Nevertheless, the precise mechanisms underlying turnover of most of the proteasome substrates that are regulated in both Ub-dependent and Ub-independent manners are not well understood. To our knowledge, the HCV core protein is the first

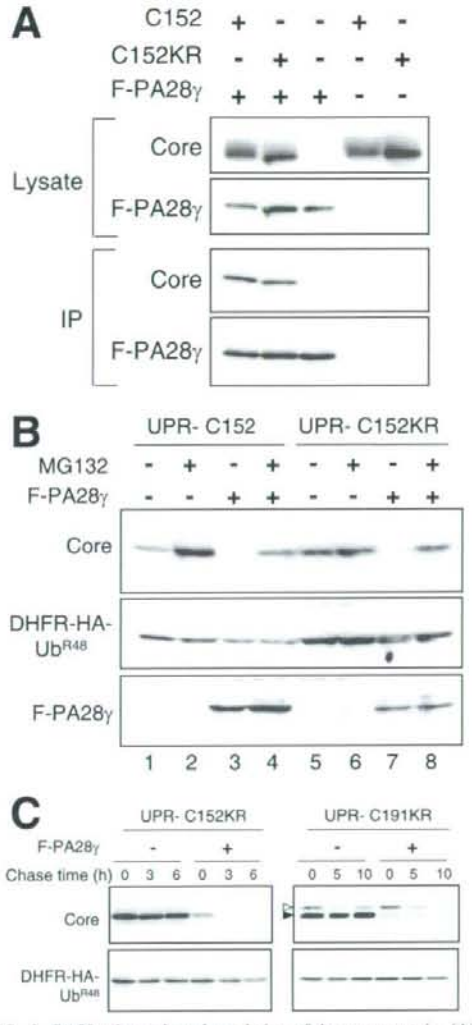

FIG. 3. PA28γ-dependent degradation of the core protein. (A) Interaction of the core protein with PA28γ. Cells were cotransfected with the wild-type (C152) or Lys-less (C152KR) core expression plasmid in the presence of a Flag-PA28γ (F-PA28γ) expression plasmid or an empty vector. The transfected cells were treated with MG132. After 48 h, the cell lysates were immunoprecipitated with anti-Flag antibody and visualized by Western blotting with anticore antibodies. Western blot analysis of whole cell lysates was also performed. (B) Degradation of the wild-type and Lys-less core proteins via the PA28γ-dependent pathway. Cells were transfected with the UPR construct with or without F-PA28γ. In some cases, cells were treated with 10 μM MG132 for 14 h before harvesting. Western blot analysis was performed using anticore, anti-HA, and anti-Flag antibodies. (C) After 24 h of transfection with UPR-C152KR and UPR-C191KR with or without F-PA28γ (an empty vector), cells were treated with 50 μg of cycloheximide/ml for different time periods as indicated (chase time). Western blot analysis was performed using anticore and anti-HA antibodies. The precursor core protein and the core that was processed, presumably by signal peptide peptidase, are denoted by open and closed triangles, respectively.

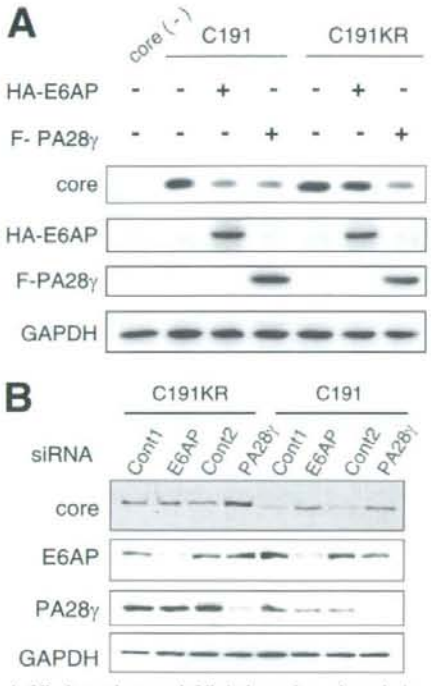

FIG. 4. Ub-dependent and Ub-independent degradation of the full-length core protein in hepatic cells. (A) Huh-7 cells were cotransfected with plasmids for the full-length core protein (C191) or its Lys-less mutant (C191KR) in the presence of F-PA28γ or HA-tagged-E6AP expression plasmid (HA-E6AP). After 48 h, cells were lysed and Western blot analysis was performed using anticore, anti-HA, anti-Flag, or anti-GAPDH. (B) Huh-7 cells were cotransfected with core expression plasmids along with siRNA against PA28γ or E6AP or with negative control siRNA. Cells were harvested 72 h after transfection and subjected to Western blot analysis.

viral protein studied that has led to identification of key cellular factors responsible for proteasomal degradation via dual distinct mechanisms. Although the question remains whether there is a physiological significance of the Ub-dependent and Ub-independent degradation of the core protein, it is reasonable to consider that tight control over cellular levels of the core protein, which is multifunctional and essential for viral replication, maturation, and pathogenesis, may play an important role in representing the potential for its functional activity.

This work was supported by a grant-in-aid for Scientific Research from the Japan Society for the Promotion of Science, from the Ministry of Health, Labor and Welfare of Japan, and from the Ministry of Education, Culture, Sports, Science and Technology, by Research on Health Sciences focusing on Drug Innovation from the Japan Health Sciences Foundation, Japan, and by the Program for Promotion of Fundamental Studies in Health Sciences of the National Institute of Biomedical Innovation of Japan.

REFERENCES

1. **Asher, G., J. Lotem, L. Sachs, C. Kahana, and Y. Shaul.** 2002. Mdm-2 and ubiquitin-independent p53 proteasomal degradation regulated by NQO1. Proc. Natl. Acad. Sci. USA **99:**13125–13130.
2. **Asher, G., P. Tsvetkov, C. Kahana, and Y. Shaul.** 2005. A mechanism of ubiquitin-independent proteasomal degradation of the tumor suppressors p53 and p73. Genes Dev. **19:**316–321.
3. **Chen, X., L. F. Barton, Y. Chi, B. E. Clurman, and J. M. Roberts.** 2007. Ubiquitin-independent degradation of cell-cycle inhibitors by the REGγ proteasome. Mol. Cell **26:**843–852.
4. **Ciechanover, A.** 1998. The ubiquitin-proteasome pathway: on protein death and cell life. EMBO J. **17:**7151–7160.
5. **Hershko, A., A. Ciechanover, and A. Varshavsky.** 2000. The ubiquitin system. Nat. Med. **6:**1073–1081.
6. **Jariel-Encontre, I., M. Pariat, F. Martin, S. Carillo, C. Salvat, and M. Piechaczyk.** 1995. Ubiquitinylation is not an absolute requirement for degradation of c-Jun protein by the 26 S proteasome. J. Biol. Chem. **270:**11623–11627.
7. **Jin, Y., H. Lee, S. X. Zeng, M. S. Dai, and H. Lu.** 2003. MDM2 promotes p21waf1/cip1 proteasomal turnover independently of ubiquitylation. EMBO J. **22:**6365–6377.
8. **Ju, D., and Y. Xie.** 2006. Identification of the preferential ubiquitination site and ubiquitin-dependent degradation signal of Rpn4. J. Biol. Chem. **281:**10657–10662.
9. **Lai, M. M. C., and C. F. Ware.** 1999. Hepatitis C virus core protein: possible roles in viral pathogenesis. Springer, Berlin, Germany.
10. **Lévy, F., N. Johnsson, T. Rumenapf, and A. Varshavsky.** 1996. Using ubiquitin to follow the metabolic fate of a protein. Proc. Natl. Acad. Sci. USA **93:**4907–4912.
11. **Li, X., L. Amazit, W. Long, D. M. Lonard, J. J. Monaco, and B. W. O'Malley.** 2007. Ubiquitin- and ATP-independent proteolytic turnover of p21 by the REGγ-proteasome pathway. Mol. Cell **26:**831–842.
12. **Li, X., D. M. Lonard, S. Y. Jung, A. Malovannaya, Q. Feng, J. Qin, S. Y. Tsai, M. J. Tsai, and B. W. O'Malley.** 2006. The SRC-3/AIB1 coactivator is degraded in a ubiquitin- and ATP-independent manner by the REGγ proteasome. Cell **124:**381–392.
13. **Liu, Q., C. Tackney, R. A. Bhat, A. M. Prince, and P. Zhang.** 1997. Regulated processing of hepatitis C virus core protein is linked to subcellular localization. J. Virol. **71:**657–662.
14. **Lonard, D. M., Z. Nawaz, C. L. Smith, and B. W. O'Malley.** 2000. The 26S proteasome is required for estrogen receptor-α and coactivator turnover and for efficient estrogen receptor-α transactivation. Mol. Cell **5:**939–948.
15. **Moradpour, D., F. Penin, and C. M. Rice.** 2007. Replication of hepatitis C virus. Nat. Rev. Microbiol. **5:**453–463.
16. **Moriishi, K., R. Mochizuki, K. Moriya, H. Miyamoto, Y. Mori, T. Abe, S. Murata, K. Tanaka, T. Miyamura, T. Suzuki, K. Koike, and Y. Matsuura.** 2007. Critical role of PA28γ in hepatitis C virus-associated steatogenesis and hepatocarcinogenesis. Proc. Natl. Acad. Sci. USA **104:**1661–1666.
17. **Moriishi, K., T. Okabayashi, K. Nakai, K. Moriya, K. Koike, S. Murata, T. Chiba, K. Tanaka, R. Suzuki, T. Suzuki, T. Miyamura, and Y. Matsuura.** 2003. Proteasome activator PA28γ-dependent nuclear retention and degradation of hepatitis C virus core protein. J. Virol. **77:**10237–10249.
18. **Niwa, H., K. Yamamura, and J. Miyazaki.** 1991. Efficient selection for high-expression transfectants with a novel eukaryotic vector. Gene **108:**193–199.
19. **Realini, C., C. C. Jensen, Z. Zhang, S. C. Johnston, J. R. Knowlton, C. P. Hill, and M. Rechsteiner.** 1997. Characterization of recombinant REGα, REGβ, and REGγ proteasome activators. J. Biol. Chem. **272:**25483–25492.
20. **Santolini, E., G. Migliaccio, and N. La Monica.** 1994. Biosynthesis and biochemical properties of the hepatitis C virus core protein. J. Virol. **68:**3631–3641.
21. **Sheaff, R. J., J. D. Singer, J. Swanger, M. Smitherman, J. M. Roberts, and B. E. Clurman.** 2000. Proteasomal turnover of p21Cip1 does not require p21Cip1 ubiquitination. Mol. Cell **5:**403–410.
22. **Shirakura, M., K. Murakami, T. Ichimura, R. Suzuki, T. Shimoji, K. Fukuda, K. Abe, S. Sato, M. Fukasawa, Y. Yamakawa, M. Nishijima, K. Moriishi, Y. Matsuura, T. Wakita, T. Suzuki, P. M. Howley, T. Miyamura, and I. Shoji.** 2007. E6AP ubiquitin ligase mediates ubiquitylation and degradation of hepatitis C virus core protein. J. Virol. **81:**1174–1185.
23. **Suzuki, R., K. Tamura, J. Li, K. Ishii, Y. Matsuura, T. Miyamura, and T. Suzuki.** 2001. Ubiquitin-mediated degradation of hepatitis C virus core protein is regulated by processing at its carboxyl terminus. Virology **280:**301–309.
24. **Suzuki, T., and A. Varshavsky.** 1999. Degradation signals in the lysine-asparagine sequence space. EMBO J. **18:**6017–6026.
25. **Treier, M., L. M. Staszewski, and D. Bohmann.** 1994. Ubiquitin-dependent c-Jun degradation in vivo is mediated by the δ domain. Cell **78:**787–798.
26. **Wu, R. C., Q. Feng, D. M. Lonard, and B. W. O'Malley.** 2007. SRC-3 coactivator functional lifetime is regulated by a phospho-dependent ubiquitin time clock. Cell **129:**1125–1140.
27. **Zhang, Z., and R. Zhang.** 2008. Proteasome activator PA28γ regulates p53 by enhancing its MDM2-mediated degradation. EMBO J. **27:**852–864.

Biochemical and Biophysical Research Communications 377 (2008) 747–751

Contents lists available at ScienceDirect

Biochemical and Biophysical Research Communications

journal homepage: www.elsevier.com/locate/ybbrc

Characterization of infectious hepatitis C virus from liver-derived cell lines

Daisuke Akazawa [a,b], Tomoko Date [b], Kenichi Morikawa [b], Asako Murayama [b], Noriaki Omi [a,b], Hitoshi Takahashi [a,b], Noriko Nakamura [a], Koji Ishii [b], Tetsuro Suzuki [b], Masashi Mizokami [c], Hidenori Mochizuki [a], Takaji Wakita [b,*]

[a] Pharmaceutical Research Laboratories, Toray Industries, Inc., Kanagawa, Japan
[b] Department of Virology II, National Institute of Infectious Diseases, 1-23-1 Toyama, Shinjuku-ku, Tokyo 162-8640, Japan
[c] Department of Clinical Molecular Informative Medicine, Nagoya City University Graduate School of Medical Sciences, Nagoya, Japan

ARTICLE INFO

Article history:
Received 20 September 2008
Available online 23 October 2008

Keywords:
Cell culture
Hepatitis C virus
Infectivity
Particle
Replicon

ABSTRACT

The efficient production of infectious HCV from the JFH-1 strain is restricted to the Huh7 cell line and its derivatives. However, the factors involved in this restriction are unknown. In this study, we examined the production of infectious HCV from other liver-derived cell lines, and characterized the produced viruses. Clones of the Huh7, HepG2, and IMY-N9, harboring the JFH-1 full-genomic replicon, were obtained. The supernatant of each cell clone exhibited infectivity for naive Huh7. Each infectious supernatant was then characterized by sucrose density gradient. For all of the cell lines, the main peak of the HCV-core protein and RNA exhibited at approximately 1.15 g/mL of buoyant density. However, the supernatant from the IMY-N9 differed from that of Huh7 in the ratio of core:RNA at 1.15 g/mL and significant peaks were also observed at lower density. The virus particles produced from the different cell lines may have different characteristics.

Hepatitis C virus (HCV) is an enveloped virus that belongs to the *Hepacivirus* genus of the *Flaviviridae* family. HCV is a human pathogen and HCV infection is a major cause of chronic hepatitis, liver cirrhosis and hepatic carcinoma. The main therapy for HCV is treatment with pegylated-interferon and rivabirin. However, these agents show little effect for patients that have a high titer of HCV-RNA, genotype 1. Thus, it is necessary to develop new, more effective therapies and preventive treatments to counteract HCV infection. It was discovered that a genotype 2a strain of HCV, JFH-1, can efficiently replicate in the Huh7 cell line [1], and an *in vitro* culture model of infectious HCV has also been successfully developed using the JFH-1 genome [2–4]. Recently, it has become possible to produce various chimeric HCV by replacement of the JFH-1 structural protein region with that of other strains. The HCV particles produced from such chimera are expected to lead to the development of a HCV vaccine, and new anti-HCV pharmaceuticals.

The infectious HCV-derived JFH-1 genome was developed using the human hepatoma Huh7 cell line [5]. Although the sub-genomic replicon RNA of JFH-1 can autonomously replicate, not only in Huh7 cells, but in other human liver [6], non-hepatic [7], and mouse [8] cells, infectious HCV production has been restricted to Huh7-derived cells. In this study, we undertook a comparative study of infectious HCV particles produced from different cell lines including Huh7. Infectious HCV particles were successfully produced into the culture media and characterized.

* Corresponding author. Fax: +81 3 5285 1161.
E-mail address: wakita@nih.go.jp (T. Wakita).

0006-291X/$ - see front matter © 2008 Elsevier Inc. All rights reserved.
doi:10.1016/j.bbrc.2008.10.063

Materials and methods

Cell culture. Huh7, Huh7.5.1 ([3], a generous gift from Dr. Francis V. Chisari), HepG2, and IMY-N9 cells were cultured at 37 °C in 5% CO_2. The HepG2 cells were cultured in modified Eagle's medium containing 10% fetal bovine serum. All of the other cells were cultured in Dulbecco's modified Eagle's medium containing 10% fetal bovine serum, as described previously [6].

Plasmids. The pFGR-JFH1 and pFGR-JFH1/deltaE12 plasmids, encoding the full-genomic replicon, and envelope-deleted replicons, respectively, were generated as previously described [9].

RNA synthesis. RNA synthesis was performed as described previously [2]. Briefly, the pFGR-JFH1 plasmid was digested with XbaI and then treated with Mung Bean nuclease (New England Biolabs, Beverly, MA). The digested plasmid DNA fragment was then purified and used as a template for RNA synthesis. HCV-RNA was synthesized *in vitro* using a MEGAscript™ T7 kit (Ambion, Austin, TX). The synthesized RNA was treated with DNaseI, followed by acid phenol extraction to remove any remaining template DNA.

Establishment of replicon cells. Cell lines harboring FGR-JFH1 replicons were produced as described previously [9]. Briefly, trypsinized cells were washed with Opti-MEM I™ reduced-serum medium (Invitrogen, Carlsbad, CA) and resuspended at 7.5×10^6 cells/mL with Cytomix buffer [1]. RNA (10 μg), synthesized from pFGR-JFH1, was mixed with 400 μL of cell suspension and transferred to an electroporation cuvette (Precision Universal Cuvettes, Thermo Hybrid, Middlesex, UK). The cells were then pulsed at 260 V and 950 μF with the Gene Pulser II™ apparatus (Bio-Rad,

Hercules, CA). Transfected cells were immediately transferred to 10-cm culture dishes, each containing 8 mL of culture medium. G418 (0.8–1.0 mg/mL) (Nacalai Tesque, Kyoto, Japan) was added to the culture medium at 16–24 h after transfection. Culture medium, supplemented with G418, was replaced twice per week. Three weeks after transfection, sparsely grown G418-resistant colonies were independently isolated using a cloning cylinder (Asahi Techno Glass Co., Tokyo, Japan), and were expanded.

Preparation of supernatants from FGR-JFH1 replicon cells. Culture media was collected from Huh7, IMY-N9, and HepG2 cell lines harboring the FGR-JFH1 replicon and was passed through a 0.45-μm filter. Filtrated culture media was then pooled and concentrated 50-fold using Amicon Ultra-15 (100,000 Molecular weight cut off; Millipore, Bedford, MA), and stored at −80 °C until use.

Assay of infection of naïve Huh7 cells. Infection of naïve Huh7 cells were assayed by immunofluorescence and colony formation assays. For the immunofluorescence assay naïve Huh7.5.1 cells were seeded at 1×10^4 cells/well in an 8-well chamber slide (Becton Dickinson, Franklin Lakes, NJ), cultured overnight and then inoculated with diluted culture media containing infectious HCV particles (1×10^6 HCV-RNA copies). At 72 h after inoculation, the cells were fixed in acetone/methanol (1:1) for 10 min at −20 °C, and the infected foci were visualized by immunofluorescence as follows.

An anti-core HCV protein monoclonal antibody 2H9 [2] was added to the cells at 50 μg/mL in BlockAce (Dainippon Sumitomo Pharma, Osaka, Japan). After incubation for 1 h at room temperature, the cells were washed and incubated with a 1:400 dilution of AlexaFluor 488-conjugated anti-mouse IgG (Molecular Probes, Eugene, OR) diluted in BlockAce. The cells were then washed, treated with DAPI solution (Sigma, Saint Louis, MO) at 0.1 μg/mL and examined by Biozero fluorescence microscopy (Keyence, Osaka, Japan).

Colony formation assays were performed as described previously [9]. Briefly, naïve Huh7 cells were inoculated with culture supernatants from replicon-expressing cell lines for 2 h, and then cultured with complete medium. Inoculated cells were cultured for 3 weeks in medium supplemented with G418 (0.3 mg/mL). Cell survival was assessed by staining with crystal violet.

Titration of infectivity. The infectivity titer of the culture supernatants was determined on Huh7.5.1 cells by end point dilution and immunofluorescence as described above. Briefly, each sample was serially diluted 10-fold in DMEM-10% FBS and 100 μL was used to inoculate Huh7.5.1 cells. Infection was examined 72 h post-inoculation by immunofluorescence using a mouse monoclonal anti-core antibody and secondary anti-mouse IgG-Alexa 488 conjugated antibodies. Infectious foci were counted and the titer was calculated and expressed as focus forming units per mL (FFU/mL).

Sucrose density gradient analysis. Concentrated cell supernatants were layered on top of a preformed continuous 10–60% sucrose gradient in TNE buffer containing 10 mM Tris, pH7.5, 150 mM NaCl, and 0.1 mM EDTA. Gradients were centrifuged in an SW41 rotor (Beckman Coulter, Fullerton, CA) at 35,000 rpm for 16 h at 4 °C, and fractions (400 μL each) were collected from the bottom of the tube. The density of each fraction was estimated by weighing a 100 μL drop from each fraction following a gradient run.

Quantification of HCV-core protein and RNA. The level of the HCV-core protein in culture supernatants or sucrose density gradient fractions, was assayed using an immunoassay as described elsewhere [10]. Viral RNA was isolated from harvested culture media, or sucrose density gradient fractions, using the QiaAmp Viral RNA Extraction kit (Qiagen, Tokyo, Japan). The copy number of HCV RNA was determined by real-time detection reverse transcription-polymerase chain reaction (RTD-PCR), using an ABI Prism 7500fast sequence detector system (Applied Biosystems, Tokyo, Japan) [11].

Results

Production of infectious HCV from human liver-derived cell lines

We first determined if it was possible to produce infectious HCV from cell lines other than Huh7. We selected the HepG2 and IMY-N9 cell lines to establish human liver-derived cell lines that enable replication of the JFH-1 genome [6]. Since full-genomic JFH-1 did not transiently replicate in these cells (data not shown), we established FGR-JFH1 replicon cells that stably replicate the JFH-1 genome. In the culture media obtained from these full-genomic replicon cells, HCV-RNA titers were detected by RTD-PCR. The titer of HCV-RNA was highest in the supernatant from an IMY-N9 cell clone and lowest from a HepG2 cell clone (Table 1). When naïve Huh7.5.1 cells were inoculated with culture supernatants from the replicon cells, infected cells could be detected by immunofluorescence using an anti-HCV-core protein antibody (Fig. 1A). These data suggested that HepG2 and IMY-N9 cells are able to produce infectious HCV.

We then compared the specific infectivity of the replicon containing culture supernatants from the different cells. Specific infectivity was calculated by dividing the infectious titer, calculated by immunofluorescence of infectious foci, of the culture media by the titer obtained for HCV-RNA. Using these calculations the culture media from Huh7 and HepG2 cells showed almost the same specific infectivity whereas that from IMY-N9 cell was relatively higher (Table 1). Thus the infectious HCV in the culture media might differ according to the cell line from which it was obtained.

To clarify the differences observed in specific infectivity, we next examined the ability of the various cellular supernatants to induce colony formation. For this assay naïve Huh7 cells were inoculated with culture media of the same HCV-RNA titer as that of the FGR-JFH1 virus and were cultured in G418-containing medium. Cell survival was assayed by staining with crystal violet, and the number of colonies formed was counted. Consistent with the specific infectivity results, the supernatant of the IMY-N9 replicon cell showed higher colony formation compared with that of Huh7 and HepG2 replicon cells (Fig. 1B and C). Thus IMY-N9 cells produce infectious HCV with a relatively higher infectivity than the other cell lines suggesting that the supernatant derived from the different replicon producing cells may differ.

Characterization of the FGR-JFH1 virus from different liver-derived cells

To further characterize potential differences between the viruses produced by the different cell lines we next characterized the FGR-JFH1 virus in the media of the different cell lines by sucrose density gradient analysis. Concentrated cell supernatants were layered on top of a preformed continuous 10–60% sucrose gradient and centrifuged. Twenty-four fractions were collected and the HCV-core protein and RNA was assayed in each fraction. The peak fraction of the HCV-core protein and that of the RNA coincided at a density of 1.15 g/mL in all supernatants. However, the supernatant of the IMY-N9 cells showed different profiles for both the HCV-core protein and RNA compared to those of Huh7. Thus the IMY-N9 cells had a different ratio of

Table 1
Infectivity of the supernatant of replicon cell lines.

Producing cell	HCV-RNA (copies/mL)	Infectious titer (FFU/mL)	Specific infectivity (FFU/RNA copy)
Huh7	$1.36 \pm 0.02 \times 10^8$	$1.30 \pm 0.32 \times 10^4$	9.56×10^{-5}
IMY-N9	$2.80 \pm 0.04 \times 10^8$	$3.75 \pm 0.38 \times 10^4$	1.34×10^{-4}
HepG2	$8.80 \pm 0.75 \times 10^7$	$7.70 \pm 1.41 \times 10^3$	7.96×10^{-5}

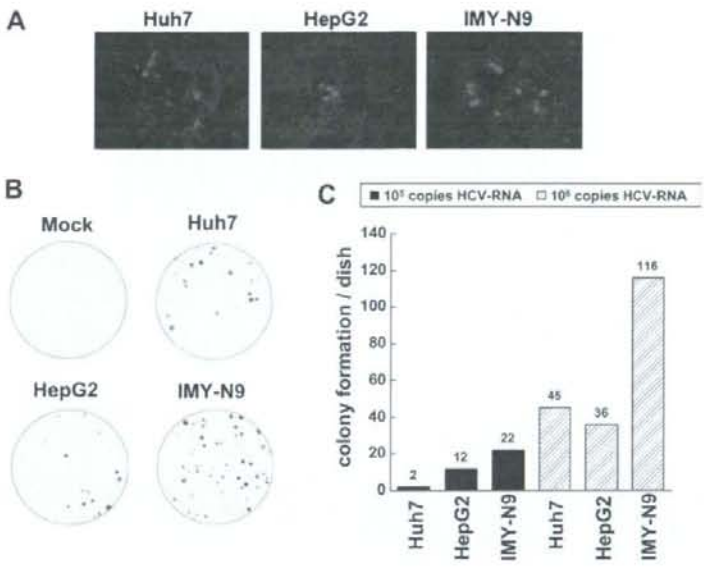

Fig. 1. Naïve Huh7 cell infection assay of JFH-1 full-genomic replicon cell culture supernatants. (A) JFH-1 full-genomic replicon (FGR-JFH1) cells were established in Huh7, HepG2, and IMY-N9 cell lines. Supernatants derived from Huh7 (*left*), HepG2 (*middle*), and IMY-N9 (*right*) cells (1×10^6 HCV-RNA copies) were inoculated into naïve Huh7.5.1 cells (1×10^4) for 48 h, and infected cells were then detected by immunofluorescence using an anti-core antibody (clone 2H9) (green). (B) Naïve Huh7 cells (5×10^5) were inoculated with mock, Huh7, HepG2, and IMY-N9-derived supernatants (10^6 HCV-RNA copies per 10-cm dish) of FGR-JFH1 cells for 2 h. Inoculated cells were cultured for 3 weeks in complete medium supplemented with G418 (0.3 mg/mL), and G418-resistant cells were stained using crystal violet. (C) The number of G418-resistant colonies obtained in (B) was calculated when 10^5 or 10^6 copies of HCV-RNA were tested. Mean values of colony number were indicated in duplicate experiment. (For interpretation of the references to color in this figure legend, the reader is referred to the web version of this article.)

HCV-core protein and RNA at a density of 1.15 g/mL (RNA/Core ratio; Huh7: 511, IMY-N9: 133 copies/fmol) and also showed a secondary peak at lower density (approximately 1.05 g/mL). For all supernatants the peak of infectivity exhibited at a density of 1.10 g/mL that was slightly lower than that of the HCV-core protein and RNA peaks. Furthermore infectivity was barely detectable in the lower density fractions (Fig. 2) suggesting that the HCV-core protein and RNA that was detected at lower density was irrelevant for infectivity of the different supernatants.

We considered the possibility that the core protein and RNA in the lighter fractions may be due to cellular debris containing a replication complex. To determine if this might be the case we therefore analyzed the supernatants from Huh7 and IMY-N9 envelope-deleted replicon cells (FGR-JFH1/deltaE12). The HCV-core protein and RNA were detected in the supernatants of these cells although the titers were very low. These supernatants were not infective for naïve Huh7 cells (data not shown). Furthermore, analysis of the concentrated supernatants of these cell lines by sucrose density gradient analysis detected both the HCV-core protein and RNA, and the major peaks of HCV-RNA were detected in the lower density (approximately 1.10 g/mL) fractions (Fig. 3). However, the profiles of HCV-core protein and RNA did not coincide for either cell line.

Discussion

Infectious HCV can be produced in cell culture by using the JFH-1 genome. This system permits investigation of various aspects of the HCV life cycle such as the steps of entry into cells, replication, and secretion. Infectious HCV derived from JFH-1 is robustly produced in Huh7 cell lines [2,3], and the infectious particles have been characterized. However the difficulty in robustly producing infectious HCV from other cell lines prevents a comparative study of HCV production among different cell lines. In this study, we compared infectious HCV production in Huh7 with that of other cell lines, and characterized the viruses produced.

First, we established Huh7, IMY-N9, and HepG2 FGR-JFH1 replicon cells. These cell lines were able to replicate the JFH-1 subgenomic replicon [6]. The HCV-core protein and RNA were detected in all of the supernatants and all of these supernatants showed infectivity for naïve Huh7. Infectivity was evaluated by transient infection and colony formation assays. These assays indicated that the infectious supernatant from IMY-N9 cell had higher infectivity than the other cell lines for naïve Huh7 cells.

Next, we characterized each supernatant by sucrose density gradient analysis, which revealed both similarities and differences among the infectious supernatants. All samples showed typical peaks at 1.15 g/mL buoyant density for HCV-core protein and RNA, and infectious fractions showed an almost identical buoyant density of 1.10 g/mL. However, the supernatant from the IMY-N9 cells showed a difference in the core/RNA ratio at a density of 1.15 g/mL and higher secondary peak of HCV-core protein and RNA at a lower density (approximately 1.05 g/mL). Since the fractions at lower density did not correlate with infectivity, it is believed that the component at lower density does not contain infectious HCV particles but rather cellular debris that contains HCV proteins, RNA, and lipids [12]. HCV can associate with lipoprotein [13,14], and is secreted with VLDL [15]. Thus, the observed differences in the HCV-producing cells may derive from differences in lipoprotein synthesis. However, it is also possible that the components migrating at lower density contain virus particles. The deletion mutant of FGR-JFH1 (FGR-JFH1/deltaE12) did replicate in Huh7 and IMY-N9 cells, and these replicon cells secreted the HCV-core protein into the culture media, although at low levels. HCV-RNA was also detected in the same culture medium, and the profile of this HCV-RNA differed from that of the HCV-core protein in sucrose density gradient analysis. Thus, the

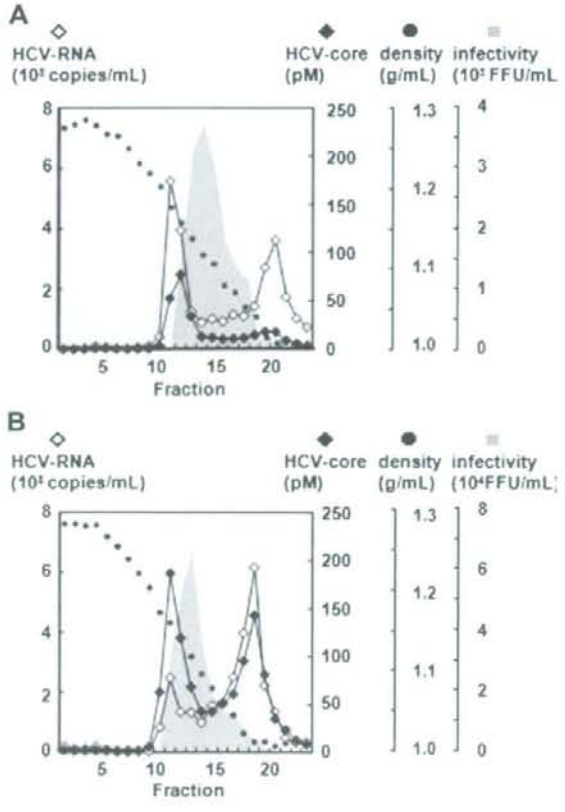

Fig. 2. Density gradient analysis of infectious HCV derived from Huh7 and IMY-N9 cells. Concentrated supernatants of Huh7 cells (A) and IMY-N9 cells (B) were layered on top of a preformed continuous 10–60% sucrose gradient in TNE buffer. The gradients were centrifuged in a SW41 rotor at 35,000 rpm for 16 h at 4 °C, and fractions (400 μL each) were collected from the bottom of the tube. The buoyant density (closed circles), HCV-core protein (closed diamonds), HCV-RNA (open diamonds) and infectivity for naïve Huh7.5.1 cells (shown in gray) was detected in each fraction as described in Materials and methods.

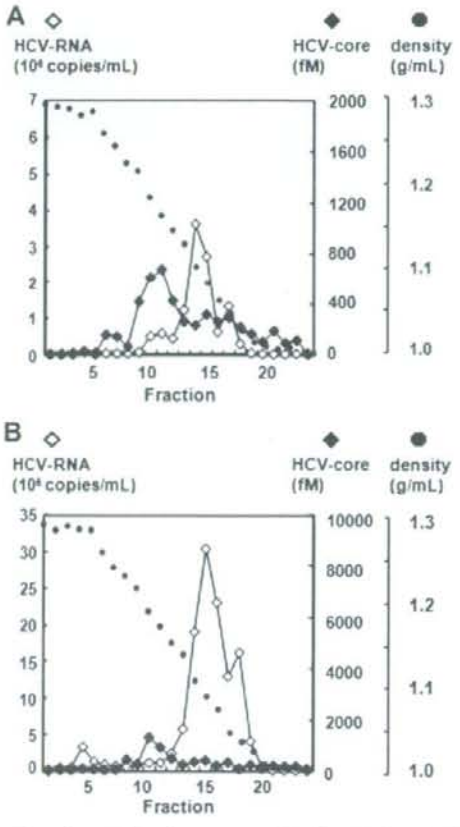

Fig. 3. Density gradient analysis of supernatants derived from Huh7 and IMY-N9 cells transfected with FGR-JFH1/deltaE12 RNA. Concentrated supernatants from Huh7 (A) and IMY-N9 (B) cells were analyzed by sucrose density gradient as described in the legend to Fig. 2. The buoyant density (closed circles), HCV-core protein (closed diamonds) and HCV-RNA (open diamonds) was analyzed in each fraction.

peak fractions containing the HCV-core protein and RNA from the supernatant of FGR-JFH1/deltaE12 cells were different from the peak fractions from that of FGR-JFH1 cells. Therefore it is possible that all of the peaks of HCV-core protein and RNA observed in the supernatant of FGR-JFH1 replicon cells may correlate to virus particles with different densities. However, the reason why they centrifuge at different densities is unclear. Interestingly, the supernatants from cells transfected with envelope-deleted replicon RNA exhibit non-identical HCV-core protein and RNA profiles on a sucrose density gradient. Envelope-deleted replicon RNA may have a decreased ability to form nucleocapsids although a detailed examination is necessary to establish this point.

We previously developed a method for infectious HCV production using the FGR-JFH1 [9], and have now succeeded in producing infectious HCV in the supernatant of cultured liver-derived cell lines harboring FGR-JFH1 RNA. Infectious HCV particles are useful for vaccine production and are considered good antigens for the generation of useful antibodies. Selection of an appropriate cell line is important for the production of HCV particles for vaccine development. The technique used in this study seemed to be appropriate for producing infectious HCV in various cell lines [8].

A second advantage of using HepG2 and IMY-N9 cells for the production of virus particles is that these parental cell lines, unlike the Huh7 cell line, do not express the CD81 molecule on the cell surface, however, the expression on cell clones used in this study was not confirmed. This means that the FGR-JFH1 replicon of these cell lines may have a single cycle of HCV production, encompassing replication, assembly, budding and secretion, and do not show HCV permissiveness. These cells should therefore be useful for the discovery of drugs targeted against HCV assembly and secretion.

Acknowledgments

This work was partially supported by a grant-in-aid for Scientific Research from the Japan Society for the Promotion of Science and from the Ministry of Health, Labor, and Welfare of Japan by the Research on Health Sciences Focusing on Drug Innovation from the Japan Health Sciences Foundation. Huh7 and Huh7.5.1 was a kind gift from Dr. Francis V. Chisari.

References

[1] T. Kato, T. Date, M. Miyamoto, A. Furusaka, K. Tokushige, M. Mizokami, T. Wakita, Efficient replication of the genotype 2a hepatitis C virus subgenomic replicon, Gastroenterology 125 (2003) 1808–1817.

[2] T. Wakita, T. Pietschmann, T. Kato, T. Date, M. Miyamoto, Z. Zhao, K. Murthy, A. Habermann, H.G. Krausslich, M. Mizokami, R. Bartenschlager, T.J. Liang, Production of infectious hepatitis C virus in tissue culture from a cloned viral genome, Nat. Med. 11 (2005) 791–796.

[3] J. Zhong, P. Gastaminza, G. Cheng, S. Kapadia, T. Kato, D.R. Burton, S.F. Wieland, S.L. Uprichard, T. Wakita, F.V. Chisari, Robust hepatitis C virus infection in vitro, Proc. Natl. Acad. Sci. USA 102 (2005) 9294–9299.
[4] B.D. Lindenbach, M.J. Evans, A.J. Syder, B. Wolk, T.L. Tellinghuisen, C.C. Liu, T. Maruyama, R.O. Hynes, D.R. Burton, J.A. McKeating, C.M. Rice, Complete replication of hepatitis C virus in cell culture, Science 309 (2005) 623–626.
[5] H. Nakabayashi, K. Taketa, K. Miyano, T. Yamane, J. Sato, Growth of human hepatoma cells lines with differentiated functions in chemically defined medium, Cancer Res. 42 (1982) 3858–3863.
[6] T. Date, T. Kato, M. Miyamoto, Z. Zhao, K. Yasui, M. Mizokami, T. Wakita, Genotype 2a hepatitis C virus subgenomic replicon can replicate in HepG2 and IMY-N9 cells, J. Biol. Chem. 279 (2004) 22371–22376.
[7] T. Kato, T. Date, M. Miyamoto, Z. Zhao, M. Mizokami, T. Wakita, Nonhepatic cell lines HeLa and 293 support efficient replication of the hepatitis C virus genotype 2a subgenomic replicon, J. Virol. 79 (2005) 592–596.
[8] S.L. Uprichard, J. Chung, F.V. Chisari, T. Wakita, Replication of a hepatitis C virus replicon clone in mouse cells, Virol. J. 3 (2006) 89.
[9] T. Date, M. Miyamoto, T. Kato, K. Morikawa, A. Murayama, D. Akazawa, J. Tanabe, S. Sone, M. Mizokami, T. Wakita, An infectious and selectable full-length replicon system with hepatitis C virus JFH-1 strain, Hepatol. Res. 37 (2007) 433–443.
[10] K. Aoyagi, C. Ohue, K. Iida, T. Kimura, E. Tanaka, K. Kiyosawa, S. Yagi, Development of a simple and highly sensitive enzyme immunoassay for hepatitis C virus core antigen, J. Clin. Microbiol. 37 (1999) 1802–1808.
[11] T. Takeuchi, A. Katsume, T. Tanaka, A. Abe, K. Inoue, K. Tsukiyama-Kohara, R. Kawaguchi, S. Tanaka, M. Kohara, Real-time detection system for quantification of hepatitis C virus genome, Gastroenterology 116 (1999) 636–642.
[12] T. Pietschmann, V. Lohmann, A. Kaul, N. Krieger, G. Rinck, G. Rutter, D. Strand, R. Bartenschlager, Persistent and transient replication of full-length hepatitis C virus genomes in cell culture, J. Virol. 76 (2002) 4008–4021.
[13] M. Monazahian, S. Kippenberger, A. Muller, H. Seitz, I. Bohme, S. Grethe, R. Thomssen, Binding of human lipoproteins (low, very low, high density lipoproteins) to recombinant envelope proteins of hepatitis C virus, Med. Microbiol. Immunol. 188 (2000) 177–184.
[14] R. Thomssen, S. Bonk, C. Propfe, K.H. Heermann, H.G. Kochel, A. Uy, Association of hepatitis C virus in human sera with beta-lipoprotein, Med. Microbiol. Immunol. 181 (1992) 293–300.
[15] S.U. Nielsen, M.F. Bassendine, A.D. Burt, C. Martin, W. Pumeechockchai, G.L. Toms, Association between hepatitis C virus and very-low-density lipoprotein (VLDL)/LDL analyzed in iodixanol density gradients, J. Virol. 80 (2006) 2418–2428.

Journal of General Virology (2008), **89**, 1587–1592 DOI 10.1099/vir.0.83618-0

Short Communication

Virological characterization of the hepatitis C virus JFH-1 strain in lymphocytic cell lines

Kyoko Murakami,[1] Toshiro Kimura,[1] Motonao Osaki,[1] Koji Ishii,[1] Tatsuo Miyamura,[1] Tetsuro Suzuki,[1] Takaji Wakita[1] and Ikuo Shoji[1,2]

Correspondence
Ikuo Shoji
ishoji@med.kobe-u.ac.jp

[1]Department of Virology II, National Institute of Infectious Diseases, 1-23-1 Toyama, Shinjuku-ku, Tokyo 162-8640, Japan

[2]Division of Microbiology, Kobe University Graduate School of Medicine, 7-5-1 Kusunoki-cho, Chuo-ku, Kobe, Hyogo 650-0017, Japan

While hepatocytes are the major site of hepatitis C virus (HCV) infection, a number of studies have suggested that HCV can replicate in lymphocytes. However, *in vitro* culture systems to investigate replication of HCV in lymphocytic cells are severely limited. Robust HCV culture systems have been established using the HCV JFH-1 strain and Huh-7 cells. To gain more insights into the tissue tropism of HCV, we investigated the infection, replication, internal ribosome entry site (IRES)-dependent translation and polyprotein processing of the HCV JFH-1 strain in nine lymphocytic cell lines. HCV JFH-1 failed to infect lymphocytes and replicate, but exhibited efficient polyprotein processing and IRES-dependent translation in lymphocytes as well as in Huh-7 cells. Our results suggest that lymphocytic cells can support HCV JFH-1 translation and polyprotein processing, but may lack some host factors essential for HCV JFH-1 infection and replication.

Received 25 November 2007
Accepted 18 March 2008

Hepatitis C virus (HCV) is a major cause of chronic hepatitis, liver cirrhosis and hepatocellular carcinoma (Choo *et al.*, 1989; Saito *et al.*, 1990). Infection with HCV is frequently associated with B-cell-related diseases, such as mixed cryoglobulinaemia and non-Hodgkin's lymphoma (Hausfater *et al.*, 2000). A number of studies have suggested that HCV can replicate not only in hepatocytes, but also in lymphocytes (Ducoulombier *et al.*, 2004; Karavattathayyil *et al.*, 2000, Lerat *et al.*, 1998), whereas the determinants of HCV tropism are still unknown. The development of HCV strain JFH-1, which generates infectious HCV in culture, has made an important contribution to the study of the HCV life cycle (Lindenbach *et al.*, 2005; Wakita *et al.*, 2005; Zhong *et al.*, 2005). The HCV life cycle is divided into several steps. After entry into the cell and uncoating, the HCV life cycle leads to translation, polyprotein processing, RNA replication, virion assembly, transport and release. The JFH-1 subgenomic replicon can replicate in non-hepatic cell lines, such as HeLa cells and 293 cells, suggesting that the host factors required for HCV replication are not hepatocyte-specific (Kato *et al.*, 2005b). The SB strain of HCV (genotype 2b strain) was isolated from an HCV-infected non-Hodgkin's B-cell lymphoma and has been reported to infect B and T cells (Kondo *et al.*, 2007; Sung *et al.*, 2003). The virus titres of the SB strain in lymphocytes were, however, lower than those of JFH-1 in Huh-7 cells and the expression of HCV proteins was not confirmed (Kondo *et al.*, 2007). It is unknown whether HCV JFH-1 can infect and replicate in lymphocytes. To gain more insight into the tissue tropism of HCV infection, we investigated the infection, replication, IRES-dependent translation and polyprotein processing of the JFH-1 strain in nine lymphocytic cell lines.

We first sought to determine whether HCV JFH-1 can infect lymphocytic cell lines. We chose nine lymphocytic cell lines derived from Burkitt's lymphoma, the EBV-immortalized human B cell line, lymphoblasts and acute T-cell leukaemia. C1R, IB4, Namalwa, P3HR1 and Raji cells were Epstein–Barr virus (EBV)-positive (Table 1). Infectious HCV was generated from HCV JFH-1 RNA in Huh-7 cells (Shirakura *et al.*, 2007; Wakita *et al.*, 2005) and the calculation of the 50 % tissue culture infectious dose ($TCID_{50}$) was based on methods described previously (Lindenbach *et al.*, 2005). These cell lines (1×10^5 cells per well of a six-well plate) were incubated with 2 ml inoculum (5×10^3 or 5×10^4 $TCID_{50}$ ml^{-1}) for 3 h, washed three times with PBS, and cultured in fresh medium. The culture medium was changed every 2 days. Cells were harvested at 0 (3 h post-infection [p.i.]), 4 and 8 day p.i. HCV core antigen within cells was quantified by immunoassay (Ortho HCV-core ELISA kit; Ortho-Clinical Diagnostics). As shown in Fig. 1(a), increasing the HCV titre of the inoculum resulted in a 7.2-fold increase in the levels of HCV core protein in Huh-7 cells at 3 h p.i. Increasing the HCV titre of the inoculum resulted in a 1.5- to 3.2-fold increase in the levels of the core protein in C1R, BL41,

Table 1. Summary of the virological characterization of HCV JFH-1 in lymphocytes

Name	Source	EBV	Transfection			Concentration of G418 for selection (μg ml^{-1})	HCVcc infection	HCV-RNA replication	Translation*		Polyprotein processing†
			Buffer	Program	Efficiency				HCV-IRES	EMCV-IRES	
Bjab	Burkitt's lymphoma	−	T	T−16	>90 %	600–800	−	−	+	++	+
BL41	Burkitt's lymphoma	−	V	I−10	60–70 %	1000	−	−	+	++	ND
C1R	B lymphoblast	+	V	T−20	70–80 %	100	−	−	+++	+++	+
IB4	Lymphoblastoid	+	V	T−20	80–90 %	1000	−	−	+++	+++	+
Jurkat	Acute T cell leukaemia	−	V	I−10	60–70 %	600	−	−	++	+	ND
Namalwa	Burkitt's lymphoma	+	V	M−13	60–70 %	600–800	−	−	+++	+++	+
P3HR1	Burkitt's lymphoma	+	V	A−23	60–70 %	800	−	−	+++	+++	ND
Raji	Burkitt's lymphoma	+	V	T−27	70–80 %	800	−	−	++	+++	+
Ramos	Burkitt's lymphoma	−	V	M−13	40–60 %	400	−	−	+	+	ND
Huh7	Hepatoma	−	T	T−14	70–80 %	500	+	+	+++	+++	+

*+, <0.25 fold IRES activity of Huh-7; ++, 0.25–0.75 fold; +++, 0.75–1.5-fold; ++++, >1.5-fold.
†ND, Not determined.

Fig. 1. HCV infection assay. (a) HCV core protein levels 3 h after infection. A total of 1×10^5 cells were infected with 2 ml of the inoculum (5×10^3 [white bars] or 5×10^4 [grey bars] $TCID_{50}$ ml^{-1}) for 3 h at 37 °C and harvested at 3 h p.i. HCV core protein in cell lysate was quantified by ELISA. The average values with standard deviations from triplicate samples are shown. The cut-off value of the immunoassay is indicated by an arrow and a dotted line. The difference between low m.o.i. (white bars) and high m.o.i. (grey bars) was significant (*, $P<0.05$; **, $P<0.01$, Student's *t*-test). (b) Time-course of HCV core protein levels after infection. In total, 1×10^5 cells were infected with 2 ml of the inoculum (5×10^3 [a] or 5×10^4 [b] $TCID_{50}$ ml^{-1}) for 3 h and harvested at 0, 4 and 8 days p.i. HCV core protein in cell lysate was quantified by ELISA. Average values ± SD from triplicate samples are shown.

P3HR1 and Raji cells, suggesting that HCV can bind to these cell lines (Fig. 1a). In contrast, the levels of HCV core protein in IB4, Jurkat and Ramos cells at 3 h p.i. were below the detection limits and there were no significant differences in the levels of the core protein in Bjab cells and Namalwa cells, suggesting that HCV binding to these cells was very inefficient (Fig. 1a). Moreover, the levels of HCV core protein increased in Huh-7 cells but, in the case of all lymphocytic cell lines, including Raji cells, the core titre did not increase at day 4 and 8 p.i., suggesting that HCV JFH-1 does not infect and/or replicate efficiently in these lymphocytic cell lines (Fig. 1b).

To assess the replication of JFH-1 in our lymphocytic cell lines, we utilized the HCV replicon system. To visualize the

replicating cells, a reporter replicon plasmid was constructed as follows. The gene encoding green fluorescence protein (GFP) was fused to the neomycin resistance gene using an overlap PCR amplification technique and the fusion product was inserted into pSGR-JFH1. The resultant plasmid was pSGR-GFPneo-JFH1. This plasmid was linearized with *XbaI* and used as a template for *in vitro* transcription using an AmpliScribe T7 High Yield Transcription kit (Epicentre Biotechnologies). RNA was transfected with high transfection efficiency and low cytotoxicity using the Nucleofector system (Amaxa Biosystems) (Coughlin *et al.*, 2004; Miyahara *et al.*, 2005; Van De Parre *et al.*, 2005). The transfection efficiencies ranged from 60 to 80 % after optimization of transfection conditions (Table 1). GFP expression was monitored periodically during the selection of HCV-replicon cells by G418 (Table 1). The GFP-expressing cells were detected at day 3 post-transfection (p.t.) in Huh-7, P3HR1, Raji, C1R and Namalwa cells. The rate of GFP expression in Huh-7 cells was more than 50 %. The rate of GFP-expression in lymphocytic cell lines was less than 1 %, despite the high transfection efficiencies. After 3 weeks of G418 selection, SGR-GFPneo-JFH1 replicon cells were established in Huh-7 cells, but not in lymphocytic cells. These data suggest that JFH-1 subgenomic replicon RNA cannot replicate in the lymphocytic cell lines.

To facilitate quantification of replication, we performed luciferase assays using subgenomic replicon RNA (SGR-JFH1/Luc) carrying firefly luciferase as a reporter. SGR-JFH1/Luc RNA was *in vitro*-transcribed using the linearized pSGR-JFH1/Luc (Kato *et al.*, 2005a) as template DNA. Cells were harvested at 4, 24, 48 and 72 h p.t. and luciferase activities were assayed with luciferase assay reagent (Promega). Assays were performed at least in triplicate. There were significant differences in luciferase activities at 4 h p.t. among the cell lines, probably because there were differences in transfection efficiencies and the doubling time of the cell lines. Thus, the replication activity was expressed relative to the reporter activity determined 4 h p.t. for each cell line, which was set to 1 (Fig. 2a). HCV subgenomic replicon RNA efficiently replicated in Huh-7 cells (Fig. 2a). Replication-deficient subgenomic replicon RNA encoding a GDD to GND mutation in NS5B served as a negative control in Huh-7 cells. The luciferase activities of replication-deficient subgenomic replicon RNA in lymphocytic cell lines also decreased rapidly (data not shown). As shown in Fig. 2(a), the luciferase activities of HCV subgenomic replicon RNA in lymphocytic cell lines decreased rapidly, suggesting that HCV subgenomic replicon RNA did not replicate efficiently in lymphocytic cell lines. Thus, these two different replicon assays demonstrated that the HCV JFH-1 subgenomic replicon failed to replicate in our lymphocytic cell lines.

To determine which steps of the HCV life cycle are impaired, we further examined translation and polyprotein processing. At first, we assessed HCV IRES-dependent translational efficiencies in the lymphocytic cell lines. Cells were co-transfected with the subgenomic replicon RNA (SGR-JFH1/Luc) and a capped RNA encoding *Renilla* luciferase (cap-luc). Cap-luc RNA was *in vitro*-transcribed using a T7 mMessage mMachine kit (Ambion). The HCV IRES activities in IB4, Namalwa and P3HR1 cells were as high as in Huh-7 cells. The HCV IRES activities in Jurkat and Raji cells were about 50 % of those in Huh-7 cells, and the HCV IRES activities in Bjab, BL41 and Ramos cells were less than 25 % of those in Huh-7 cells. On the other hand, the HCV IRES activity in C1R cells was about twofold higher than in Huh-7 cells (Fig. 2b). Replication-deficient subgenomic replicon RNA encoding a GDD to GND mutation in NS5B showed a luciferase activity level similar to that of the wild-type, suggesting that the luciferase activity at 4 h after transfection reflected translational levels but not replication levels (data not shown). Our data indicate high HCV IRES activities in all cell lines, except in Bjab, BL41 and Ramos.

The HCV polyprotein is translated in subgenomic replicon cells in an encephalomyocarditis virus (EMCV) IRES-dependent manner. To rule out the possibility that the EMCV IRES-dependent translation is impaired in lymphocytic cell lines, we assessed the EMCV IRES-dependent translational efficiencies. We assayed EMCV IRES activity using EMCV IRES-driven luciferase RNA (EMC-luc) and Cap-luc RNA. The EMCV IRES activity was five- to tenfold higher in C1R, Namalwa, IB4 and P3HR1 than in Huh-7 cells (Fig. 2c). From these results, HCV IRES and EMCV IRES exhibited sufficient translational activity in C1R, Namalwa, P3HR1 and Raji cells, suggesting that IRES-dependent translation was not impaired in these lymphocytic cell lines.

To determine whether HCV polyprotein is properly processed in lymphocytes, we examined the processing of HCV non-structural (NS) proteins. The construct pSGR-JFH1/Luc expresses the polyprotein NS3-NS4A-NS4B-NS5A-NS5B. The HCV NS3/4A protease is responsible for proteolytic processing at each cleavage site. We used the eukaryotic transient-expression system based on a recombinant vaccinia virus carrying bacteriophage T7 RNA polymerase (T7vac) (Fuerst *et al.*, 1989). To express the SGR-JFH1/Luc encoding HCV NS proteins, 5×10^6 cells were transfected with 5 μg pSGR-JFH1/Luc and infected with 2.5×10^9 p.f.u. T7vac, harvested at 24 h p.i., and analysed by Western blotting. Completely processed NS3, NS5A and NS5B proteins were detected in Bjab, Raji, IB4 and Namalwa cells as well as in pSGR-JFH1/Luc-transfected Huh-7 cells and HCV-JFH1-infected Huh-7 cells (Fig. 2c). The unprocessed polyprotein was not detected by immunoblotting in these lymphocytic cell lines (data not shown). These results suggest that the HCV polyprotein is efficiently processed in these lymphocytic cells.

In this study, we demonstrated that HCV JFH-1 failed to infect and replicate in nine lymphocytic cell lines. In contrast, HCV IRES-dependent translation and polyprotein processing by NS3/NS4A protease functioned properly

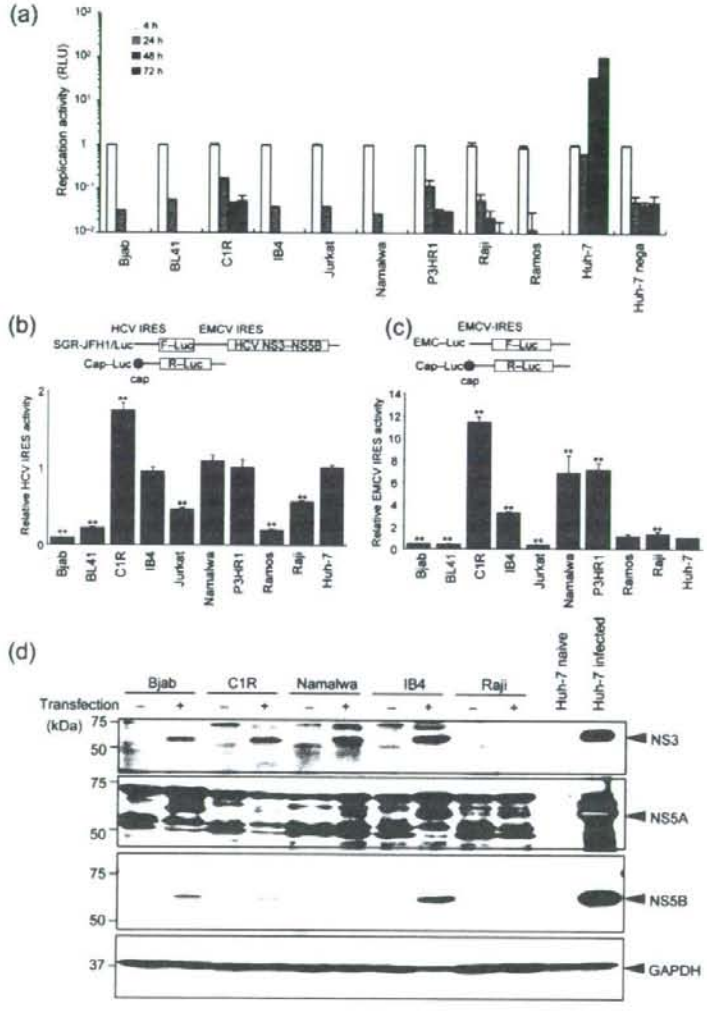

Fig. 2. Replication, HCV IRES-dependent translational efficiencies and polyprotein processing. (a) Subgenomic replicon assay. JFH-1 subgenomic replicon RNA was transfected into several cell lines and harvested at 4, 24, 48 and 72 h p.t. The replication activity was expressed relative to the reporter activity determined 4 h p.t. for each cell line, which was set to 1. RLU, Relative luciferase units; Huh-7 nega, Huh-7 cells transfected with SGR-JFH1/Luc GND, served as a negative control. (b) HCV IRES-dependent translational efficiency. To determine the HCV IRES activities, we co-transfected cells with SGR-JFH1/Luc RNA and Cap-Renilla luciferase RNA. The IRES activity of each cell line is expressed in relation to Huh-7 IRES activity, that is, as the ratio of HCV IRES-driven firefly luciferase activity to cap-driven *Renilla* luciferase activity. The difference in HCV IRES activity between Huh-7 cells and the lymphocytic cell line was significant (**, $P<0.01$, Student's *t*-test). (c) EMCV IRES-dependent translational efficiency. To determine the EMCV IRES activities, we co-transfected cells with EMCV–firefly luciferase RNA and Cap-Renilla luciferase RNA. The IRES activity of each cell line is expressed in relation to Huh-7 IRES activity, that is, as the ratio of EMCV IRES-driven firefly luciferase activity to cap-driven *Renilla* luciferase activity. The difference in EMCV IRES activity between Huh-7 cell and the lymphocytic cell line was significant (**, $P<0.01$, Student's *t*-test). (d) Polyprotein processing by NS3/4A protease in lymphocytic cell lines. pSGR-JFH1/Luc-transfected cells were infected with T7vac and harvested at 24 h p.i. HCV NS proteins, NS3, NS5A and NS5B were detected by using anti-NS3 rabbit polyclonal antibody (PAb), anti-NS5A rabbit PAb and anti-NS5B rabbit PAb. Arrowheads indicate the processed NS3, NS5A and NS5B proteins, respectively.

in these cells. Moreover, subgenomic replicon RNA failed to replicate in these cell lines. Our data suggest that lymphocytic cell lines may lack some host factors required for infection and replication of HCV-JFH1.

Viral entry often requires sequential interactions between viral proteins and several cellular factors. Several molecules (CD81, Claudin-1, Scavenger receptor class B member IR, LDL-receptor and glycosaminoglycans) have been reported to be involved in HCV binding and entry (Barth *et al.*, 2003; Evans *et al.*, 2007; Pileri *et al.*, 1998; Scarselli *et al.*, 2002). Further investigation will be required to clarify HCV binding and entry into lymphocytic cell lines.

HCV IRES and EMCV IRES exhibited sufficient translational activities in C1R, IB4, P3HR1, Namalwa and Raji cells. All these cell lines are EBV-positive. EBV-encoded nuclear antigen (EBNA1) has been reported to support HCV replication (Sugawara *et al.*, 1999). Two small EBV-encoded RNA species (EBERs) bind to the HCV IRES region (Wood *et al.*, 2001). These findings raise the possibility that HCV IRES activities may be modified by the EBV genome.

HCV JFH-1 subgenomic replicon RNA could not replicate in all lymphocytes tested in this study. The HCV SB strain, however, has been reported to infect Raji, Daudi, Molt-4

and Jurkat cells (Kondo *et al.*, 2007; Sung *et al.*, 2003). Still unknown is how hepatotropism and lymphotropism of HCV are determined. The GB virus B (GBV-B) is most closely related to HCV and the GBV-B infection of tamarins has been proposed as a good surrogate model for chronic hepatitis C (Bukh *et al.*, 2001; Jacob *et al.*, 2004; Lanford *et al.*, 2003; Martin *et al.*, 2003). A recent report has shown that GBV can disseminate to not only liver but also a variety of extrahepatic tissues such as haematolymphoid and genital tissues in tamarins (Ishii *et al.*, 2007). Viral RNA cloned from plasma and liver from the tamarins showed no sequence heterogeneity, suggesting that host factors determine the pleiotropism (Ishii *et al.*, 2007). It remains unclear how host factors and/or viral factors determine the tissue tropism of HCV. Further studies will be required to clarify the molecular mechanisms of HCV tissue tropism.

Acknowledgements

The authors gratefully acknowledge Drs Sanae Machida (Saitama Medical School, Saitama, Japan), Shizuko Harada (NIID, Tokyo, Japan) and Isao Hamaguchi (NIID, Tokyo, Japan) for the cell lines, and Dr Hideki Aizaki (NIID, Tokyo, Japan) for helpful discussion. This work was supported in part by grants-in-aid from the Ministry of Health, Labour and Welfare, by a grant for Research on Health Sciences focusing on Drug Innovation from the Japan Health Sciences Foundation, and by grant-in aid for young scientists (B).

References

Barth, H., Schafer, C., Adah, M. I., Zhang, F., Linhardt, R. J., Toyoda, H., Kinoshita-Toyoda, A., Toida, T., Van Kuppevelt, T. H. & other authors (2003). Cellular binding of hepatitis C virus envelope glycoprotein E2 requires cell surface heparan sulfate. *J Biol Chem* **278**, 41003–41012.

Bukh, J., Apgar, C. L., Govindarajan, S. & Purcell, R. H. (2001). Host range studies of GB virus-B hepatitis agent, the closest relative of hepatitis C virus, in New World monkeys and chimpanzees. *J Med Virol* **65**, 694–697.

Choo, Q. L., Kuo, G., Weiner, A. J., Overby, L. R., Bradley, D. W. & Houghton, M. (1989). Isolation of a cDNA clone derived from a blood-borne non-A, non-B viral hepatitis genome. *Science* **244**, 359–362.

Coughlin, C. M., Vance, B. A., Grupp, S. A. & Vonderheide, R. H. (2004). RNA-transfected CD40-activated B cells induce functional T-cell responses against viral and tumor antigen targets: implications for pediatric immunotherapy. *Blood* **103**, 2046–2054.

Ducoulombier, D., Roque-Afonso, A. M., Di Liberto, G., Penin, F., Kara, R., Richard, Y., Dussaix, E. & Feray, C. (2004). Frequent compartmentalization of hepatitis C virus variants in circulating B cells and monocytes. *Hepatology* **39**, 817–825.

Evans, M. J., von Hahn, T., Tscherne, D. M., Syder, A. J., Panis, M., Wolk, B., Hatziioannou, T., McKeating, J. A., Bieniasz, P. D. & Rice, C. M. (2007). Claudin-1 is a hepatitis C virus co-receptor required for a late step in entry. *Nature* **446**, 801–805.

Fuerst, T. R., Fernandez, M. P. & Moss, B. (1989). Transfer of the inducible *lac* repressor/operator system from *Escherichia coli* to a vaccinia virus expression vector. *Proc Natl Acad Sci U S A* **86**, 2549–2553.

Hausfater, P., Rosenthal, E. & Cacoub, P. (2000). Lymphoproliferative diseases and hepatitis C virus infection. *Ann Med Interne (Paris)* **151**, 53–57.

Ishii, K., Iijima, S., Kimura, N., Lee, Y. J., Ageyama, N., Yagi, S., Yamaguchi, K., Maki, N., Mori, K. & other authors (2007). GBV-B as a pleiotropic virus: distribution of GBV-B in extrahepatic tissues *in vivo*. *Microbes Infect* **9**, 515–521.

Jacob, J. R., Lin, K. C., Tennant, B. C. & Mansfield, K. G. (2004). GB virus B infection of the common marmoset (*Callithrix jacchus*) and associated liver pathology. *J Gen Virol* **85**, 2525–2533.

Karavattathayyil, S. J., Kalkeri, G., Liu, H. J., Gaglio, P., Garry, R. F., Krause, J. R. & Dash, S. (2000). Detection of hepatitis C virus RNA sequences in B-cell non-Hodgkin lymphoma. *Am J Clin Pathol* **113**, 391–398.

Kato, T., Date, T., Miyamoto, M., Sugiyama, M., Tanaka, Y., Orito, E., Ohno, T., Sugihara, K., Hasegawa, I. & other authors (2005a). Detection of anti-hepatitis C virus effects of interferon and ribavirin by a sensitive replicon system. *J Clin Microbiol* **43**, 5679–5684.

Kato, T., Date, T., Miyamoto, M., Zhao, Z., Mizokami, M. & Wakita, T. (2005b). Nonhepatic cell lines HeLa and 293 support efficient replication of the hepatitis C virus genotype 2a subgenomic replicon. *J Virol* **79**, 592–596.

Kondo, Y., Sung, V. M., Machida, K., Liu, M. & Lai, M. M. (2007). Hepatitis C virus infects T cells and affects interferon-gamma signaling in T cell lines. *Virology* **361**, 161–173.

Lanford, R. E., Chavez, D., Notvall, L. & Brasky, K. M. (2003). Comparison of tamarins and marmosets as hosts for GBV-B infections and the effect of immunosuppression on duration of viremia. *Virology* **311**, 72–80.

Lerat, H., Rumin, S., Habersetzer, F., Berby, F., Trabaud, M. A., Trepo, C. & Inchauspe, G. (1998). In vivo tropism of hepatitis C virus genomic sequences in hematopoietic cells: influence of viral load, viral genotype, and cell phenotype. *Blood* **91**, 3841–3849.

Lindenbach, B. D., Evans, M. J., Syder, A. J., Wolk, B., Tellinghuisen, T. L., Liu, C. C., Maruyama, T., Hynes, R. O., Burton, D. R. & other authors (2005). Complete replication of hepatitis C virus in cell culture. *Science* **309**, 623–626.

Martin, A., Bodola, F., Sangar, D. V., Goettge, K., Popov, V., Rijnbrand, R., Lanford, R. E. & Lemon, S. M. (2003). Chronic hepatitis associated with GB virus B persistence in a tamarin after intrahepatic inoculation of synthetic viral RNA. *Proc Natl Acad Sci U S A* **100**, 9962–9967.

Miyahara, Y., Naota, H., Wang, L., Hiasa, A., Goto, M., Watanabe, M., Kitano, S., Okumura, S., Takemitsu, T. & other authors (2005). Determination of cellularly processed HLA-A2402-restricted novel CTL epitopes derived from two cancer germ line genes, MAGE-A4 and SAGE. *Clin Cancer Res* **11**, 5581–5589.

Pileri, P., Uematsu, Y., Campagnoli, S., Galli, G., Falugi, F., Petracca, R., Weiner, A. J., Houghton, M., Rosa, D. & other authors (1998). Binding of hepatitis C virus to CD81. *Science* **282**, 938–941.

Saito, I., Miyamura, T., Ohbayashi, A., Harada, H., Katayama, T., Kikuchi, S., Watanabe, Y., Koi, S., Onji, M. & other authors (1990). Hepatitis C virus infection is associated with the development of hepatocellular carcinoma. *Proc Natl Acad Sci U S A* **87**, 6547–6549.

Scarselli, E., Ansuini, H., Cerino, R., Roccasecca, R. M., Acali, S., Filocamo, G., Traboni, C., Nicosia, A., Cortese, R. & Vitelli, A. (2002). The human scavenger receptor class B type I is a novel candidate receptor for the hepatitis C virus. *EMBO J* **21**, 5017–5025.

Shirakura, M., Murakami, K., Ichimura, T., Suzuki, R., Shimoji, T., Fukuda, K., Abe, K., Sato, S., Fukasawa, M. & other authors (2007).

E6AP ubiquitin ligase mediates ubiquitylation and degradation of hepatitis C virus core protein. *J Virol* **81**, 1174–1185.

Sugawara, Y., Makuuchi, M., Kato, N., Shimotohno, K. & Takada, K. (1999). Enhancement of hepatitis C virus replication by Epstein–Barr virus-encoded nuclear antigen 1. *EMBO J* **18**, 5755–5760.

Sung, V. M., Shimodaira, S., Doughty, A. L., Picchio, G. R., Can, H., Yen, T. S., Lindsay, K. L., Levine, A. M. & Lai, M. M. (2003). Establishment of B-cell lymphoma cell lines persistently infected with hepatitis C virus in vivo and in vitro: the apoptotic effects of virus infection. *J Virol* **77**, 2134–2146.

Van De Parre, T. J., Martinet, W., Schrijvers, D. M., Herman, A. G. & De Meyer, G. R. (2005). mRNA but not plasmid DNA is efficiently transfected in murine J774A.1 macrophages. *Biochem Biophys Res Commun* **327**, 356–360.

Wakita, T., Pietschmann, T., Kato, T., Date, T., Miyamoto, M., Zhao, Z., Murthy, K., Habermann, A., Krausslich, H. G. & other authors (2005). Production of infectious hepatitis C virus in tissue culture from a cloned viral genome. *Nat Med* **11**, 791–796.

Wood, J., Frederickson, R. M., Fields, S. & Patel, A. H. (2001). Hepatitis C virus 3′X region interacts with human ribosomal proteins. *J Virol* **75**, 1348–1358.

Zhong, J., Gastaminza, P., Cheng, G., Kapadia, S., Kato, T., Burton, D. R., Wieland, S. F., Uprichard, S. L., Wakita, T. & Chisari, F. V. (2005). Robust hepatitis C virus infection *in vitro*. *Proc Natl Acad Sci U S A* **102**, 9294–9299.

JOURNAL OF VIROLOGY, Aug. 2008, p. 7964–7976 Vol. 82, No. 16
0022-538X/08/$08.00+0 doi:10.1128/JVI.00826-08

Interaction of Hepatitis C Virus Nonstructural Protein 5A with Core Protein Is Critical for the Production of Infectious Virus Particles[▽]

Takahiro Masaki,[1] Ryosuke Suzuki,[1] Kyoko Murakami,[1] Hideki Aizaki,[1] Koji Ishii,[1] Asako Murayama,[1] Tomoko Date,[1] Yoshiharu Matsuura,[2] Tatsuo Miyamura,[1] Takaji Wakita,[1] and Tetsuro Suzuki[1]*

Department of Virology II, National Institute of Infectious Diseases, Shinjuku-ku, Tokyo 162-8640, Japan,[1] and Department of Molecular Virology, Research Institute for Microbial Diseases, Osaka University, Suita-shi, Osaka 565-0871, Japan[2]

Received 17 April 2008/Accepted 22 May 2008

Nonstructural protein 5A (NS5A) of the hepatitis C virus (HCV) possesses multiple and diverse functions in RNA replication, interferon resistance, and viral pathogenesis. Recent studies suggest that NS5A is involved in the assembly and maturation of infectious viral particles; however, precisely how NS5A participates in virus production has not been fully elucidated. In the present study, we demonstrate that NS5A is a prerequisite for HCV particle production as a result of its interaction with the viral capsid protein (core protein). The efficiency of virus production correlated well with the levels of interaction between NS5A and the core protein. Alanine substitutions for the C-terminal serine cluster in domain III of NS5A (amino acids 2428, 2430, and 2433) impaired NS5A basal phosphorylation, leading to a marked decrease in NS5A-core interaction, disturbance of the subcellular localization of NS5A, and disruption of virion production. Replacing the same serine cluster with glutamic acid, which mimics the presence of phosphoserines, partially preserved the NS5A-core interaction and virion production, suggesting that phosphorylation of these serine residues is important for virion production. In addition, we found that the alanine substitutions in the serine cluster suppressed the association of the core protein with viral genome RNA, possibly resulting in the inhibition of nucleocapsid assembly. These results suggest that NS5A plays a key role in regulating the early phase of HCV particle formation by interacting with core protein and that its C-terminal serine cluster is a determinant of the NS5A-core interaction.

Hepatitis C virus (HCV) infection is a major public health problem and is prevalent in about 200 million people worldwide (27, 40, 42). Current protocols for treating HCV infection fail to produce a sustained virological response in as many as half of treated individuals, and many cases progress to chronic liver disease, including chronic hepatitis, cirrhosis, and hepatocellular carcinoma (15, 31, 35, 43).

HCV is a positive-strand RNA virus classified in the *Hepacivirus* genus within the *Flaviviridae* family (55). Its approximately 9.6-kb genome is translated into a single polypeptide of about 3,000 amino acids (aa), in which the structural proteins core, E1, and E2 reside in the N-terminal region. A crucial function of core protein is assembly of the viral nucleocapsid. The amino acid sequence of this protein is well conserved among different HCV strains compared to other HCV proteins. The nonstructural (NS) proteins NS3-NS5B are considered to assemble into a membrane-associated HCV RNA replicase complex. NS3 possesses the enzymatic activities of serine protease and RNA helicase, and NS4A serves as a cofactor for NS3 protease. NS4B plays a role in the remodeling of host cell membranes, probably to generate the site for the replicase assembly. NS5B functions as the RNA-dependent RNA polymerase. NS5A is known to play an important but undefined role in viral RNA replication.

NS5A is a phosphoprotein that can be found in basally phosphorylated (56 kDa) and hyperphosphorylated (58 kDa) forms (49). Comparative sequence analyses and limited proteolysis of recombinant NS5A have demonstrated that NS5A is composed of three domains (52). Domain I is relatively conserved among HCV genotypes compared to domains II and III. Analysis of the crystal structure of the conserved domain I that immediately follows the membrane-anchoring α-helix localized at the N terminus revealed a dimeric structure (53). The interface between protein molecules is characterized by a large, basic groove, which has been proposed as a site of RNA binding. In fact, its RNA binding property has been demonstrated biochemically (17). Domains II and III of NS5A are far less understood. Domain II contains a region referred to as the interferon sensitivity determining region, and this region and its C-terminal 26 residues have been shown to be essential for interaction with the interferon-induced, double-stranded RNA-dependent protein kinase (6–10, 38, 39, 48). Domain III includes a number of potential phosphoacceptor sites and is most likely involved in basal phosphorylation. This domain tolerates insertion of large heterologous sequences such as green fluorescent protein (GFP) and is not required for function of NS5A in HCV RNA replication (1, 34). However, a study with the recently established productive HCV cell culture system using genotype 2a isolate JFH-1 (28, 56, 58) demonstrated that while insertion of GFP within the NS5A region does not affect RNA replication, it does produce marked decreases in the production of infectious virus particles (41). This suggests that the C-terminal region of NS5A may affect virus particle production independent of RNA replication. Re-

* Corresponding author. Mailing address: Department of Virology II, National Institute of Infectious Diseases, 1-23-1 Toyama, Shinjuku-ku, Tokyo 162-8640, Japan. Phone: 81 3 5285 1111. Fax: 81 3 5285 1161. E-mail: tesuzuki@nih.go.jp.

▽ Published ahead of print on 4 June 2008.